# Supplementary Information



## S1. Archaeological sites

The Murciélagos de Zuheros and Cueva de los Cuarenta caves as well as El Pirulejo site (Priego de Córdoba) are located in the Sierras Subbéticas in the Córdoba province (Andalusia), on the south-central sector of the Guadalquivir valley in southern Iberia.

The sites of Cueva de los Lagos and San Quílez are located in the mid-valley of the Ebro river and the northern Iberian Meseta, while El Portalón, at the Sierra de Atapuerca, is located in the area known as the "Corredor de la Bureba", which directly connects the northern Iberian Meseta with the Ebro river valley and thus with the Iberian Mediterranean coast. The Cueva de Los Lagos site has a similar geographical setting to El Portalón, in that it is also located in a preferential crossing area from the Ebro valley to the Northern Meseta along the Alhama river further to the east in La Rioja province. Thus, the geographic region in which the sites are found occupies a strategic location that links two of the most important Iberian fluvial valleys, Duero and Ebro, a putative entrance location for the Neolithisation of the interior of the northern Iberian plain.

### *S1.1 Murciélagos de Zuheros*

The Murciélagos de Zuheros cave is a vast cavern with over one thousand meters of speleological pathway, located at an altitude of 980m above the sea level at the northern ridge of the Cabra massif, with the opening allowing a wide view of the Guadalquivir valley. The site displays a long stratigraphic sequence from the Mid Palaeolithic to the Bronze Age.

The excavations conducted during the 60s and 70s demonstrated that the Andalusian early Neolithic, characterised by ceramics decorated *a la Almagra* (Red slip and polished surfaces) associated with a series of impressed and incised decorations (Fig. S1.1A), corresponded to the last third of the 6th millennium cal BC, thus, a chronology contemporaneous and parallel to the cultural tradition of the Western Mediterranean *Cardial* pottery. The Neolithic characterised by cardial and striated shell impressions is geographically attributed to Mediterranean Iberia, northern Morocco and the Atlantic coast of Portugal, with scarce presence in Andalusia.

The upper chambers of the Murciélagos de Zuheros cave were used as living areas from the beginning of the early Neolithic, while other deeper areas were used for funerary contexts (1). The individual analysed in this study (MUR) corresponds to a burial found in the interior of a "gour" or small lake located at the deepest chamber called "Sala de las Formaciones" approximately 80m lower with respect to the living areas (Fig. S1.1B). This burial belongs to a male in flexed position on the right side, with flexed arms over the chest and the legs bent with heels next to the pelvis. This forced position suggests that the body could have been tied up or contained in a sac or mat made from perishable material. A typical Neolithic stone bracelet and a ceramic vase with red slip and incised decorations where found as part of the burial (2). The direct radiocarbon date of this individual (7245-7025 years cal BP) confirms that he belonged to the earliest occupation phase of the cave or early Neolithic (Table S3.2).

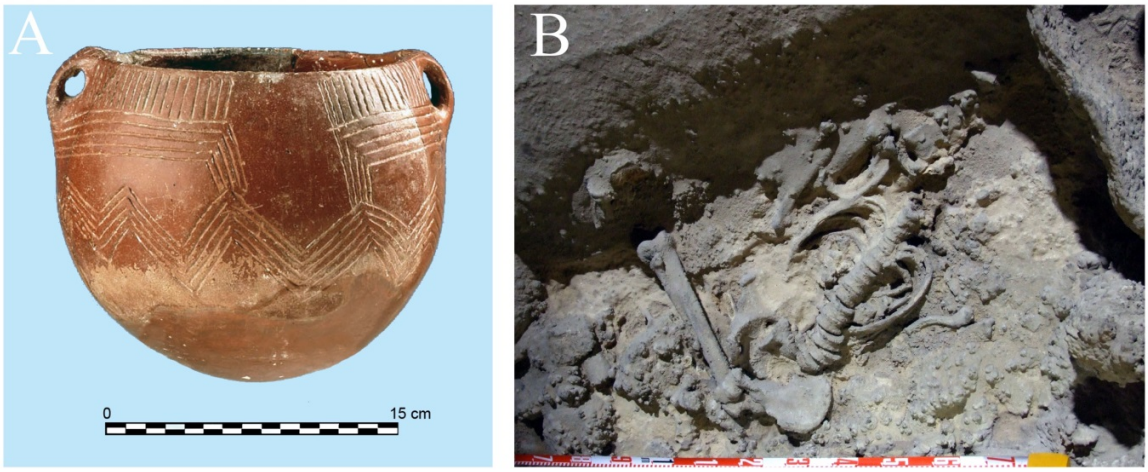


**Fig. S1.1**: **(A)** ceramics decorated a la Almagra (Red slip and polished surfaces), **(B)** burial at "Sala de las Formaciones" at Cueva de los Murciélagos.

### *S1.2 Los Cuarenta Cave*

This cave is located in the mountainous interior of the Sierras Subbéticas at 1130 metres above sea level. The cave is part of a poorly developed joint system of approximately 14m of depth. Beyond a vertical shaft of about 6m, there are different chambers that were used for collective burials during the 4th millennium cal BC (Late Neolithic).

During the archaeological survey conducted in 2007 fourteen archaeological contexts assemblies were found distributed across different chambers, locations and corridors. Altogether, these assemblies comprised the skeletal remains of at least 41 individuals represented by both females and males with a wide range of ages, from neonates to mature adults. The bodies were deposited successively at the interior of the cave, their decomposition occurred in an exposed environment, where most remains were found disarticulated (Fig. S1.2A), however, in some cases we were

able to reconstruct the successive episodes in which the burials were conducted. The burials were accompanied by scarce good graves such as stone tools, arrowheads, ceramics and few ornamental elements (3).

From the individuals analysed in this study, only the tooth obtained from skull no. 331 (C40331) yielded authentic DNA (Fig. S1.2B), This individual corresponds to a skull with no mandible that was found isolated in a small space attached to the "sala de los muertos" or chamber of the death, which is the main funeral space within the cave. This skull corresponds to a male adult with asymmetric morphology with evidence of osteomas in the parietal bones and significant dental calculus on most teeth. The direct radiocarbon date on this individual place him as the oldest within the set of chronologies obtained through radiocarbon dates for this site at 5710-5587 cal BP (table S3.2).


**Fig. S1.2**: **(A)** Deposit of bodies at the interior of the cave, **(B)** Skull No. 331 of Los Cuarenta Cave

### *S1.3 El Pirulejo*

The site of El Pirulejo (Priego de Córdoba) is a small rock shelter on a rocky cliff located in a natural internal corridor of the Andalusian Subbaetic mountains through the Arroyo Salado creek, that unlike the other two sites described above, this is located at only 580m above sea level.

The rock shelter was found in 1983 in a chance discovery and the archaeology consists mainly of Late Palaeolithic occupation layers, however the upper stratigraphic levels of the shelter, contain five episodes of funerary deposition corresponding to the Bronze Age (at approximately the middle of the second millennium cal BC). These burials were accompanied by grave goods such as ceramics and metallic ornaments as well as worked bones.

The individual analysed in this study (PIR001) is a male adult corresponding to the very first burial found at the site, interpreted as a double burial due to the findings of a second, juvenile individual. The burial was accompanied by a low angle vase which typologically was related to similar forms of the *Argar* culture (2100-1450 BC) of the Iberian southeast (4).

### *S1.4 El Portalón de Cueva Mayor*

The El Portalón cave is an archaeological site in the Sierra de Atapuerca (Burgos, Spain), a region well known for its Early and Middle Pleistocene sites (5, 6), but more recent excavations have shown that it also presents a rich and varied archaeological record (7, 8). Previous studies have successfully retrieved DNA from both humans (9, 10) and faunal (11-13) remains from the El Portalón cave.

Recent excavations at the El Portalón have revealed a stratigraphic sequence starting in the Late Pleistocene and showing evidence of human occupation throughout the Holocene. Carretero et al. (2008)(7) reported detailed radiocarbon dates for the entire stratigraphy ranging from 30,000 BP to 1,000 BP. The Holocene phase of El Portalón, includes Mesolithic, Neolithic, Chalcolithic, Bronze Age, Iron Age, Roman and Medieval periods of human occupation.

In this study we have analysed genomic data from eight individuals, either generated here for the first time (n=5; POR002, POR003, POR004, ATP5 & ATP19), or previously published (9) and complemented with new sequence data (n=3; ATP2, ATP12 & ATP16) (Table S2.1).

In addition to the site's deposits of cultural/technological and faunal remains, a series of burials have been identified in the Chalcolithic period. These burials are often accompanied with grave goods, such as pottery and animal bones in anatomical position, most commonly sheep (8). The archaeological content combined with direct radiocarbon dating of the human samples analysed suggest a pre-Bell Beaker Chalcolithic chrono-cultural assignation for the burials. Further, during the field seasons between 2015-2017, the excavation reached a Neolithic stratigraphic layer abundant with faunal remains. Excavations prior to this on disturbed sediments in the cave revealed human remains (ATP19 and ATP5) directly radiocarbon dated to the Neolithic period (see table S3.2). The Neolithic layers in El Portalón Cave appear to be related to domestic and habitation activities and no in-situ burial contexts in the Neolithic layers have been found to date. The presence of the human remains dating to this period however, implies that the cave was used as a funerary space during this time period. It is possible that the domestic activities could have disturbed previous burials, which would explain the presence of isolated and dispersed human bones within the activity floors, as observed in El Portalón during the later Chalcolithic period(8).

From the human remains from this site we have generated sequence data for 8 individuals spanning a temporal transect including the Early Neolithic (n=2) and Chalcolithic (n=6) (for the radiocarbon chronology see Table S3.2 and Fig. S3.2), that we have combined with Bronze Age data previously published (n=1) (9), enabling the study of one population at a single location over time (Fig. S1.4).


**Fig. S1.4**: Panoramic view of the archaeosedimentary sequence of the southern profile of the El Portalón site. Basal Neolithic levels have been excavated since 2015 (Unit 9). The large burial tumular limestone clast mound corresponds to pre-Bell Baker Chalcolithic (Unit 7) and Early to Late Bronze age levels constitute the thickest units (units 3 to 6) in the site. Above Bronze Age layers Iron Age to Medieval units (Units 0 to 2) are documented in different areas of the site.

### *S1.5 Cueva de los Lagos*

The Cueva de los Lagos is located in Aguilar del río Alhama, La Rioja, in northern Spain on the south bank of the Ebro River. The abundance of permeable and soluble limestone in the local geology promotes the formation of a series of wells and cavities inside the cave. Several of these interconnected cavities are responsible for the formation of lakes, in one of which the burial of the individual analysed in this study (ESP005) was found. It is possible that more than one burial occurred here, as a fragment of skull belonging to a second individual was also found. Although the human remains recovered from the interior of the cave come from uncontrolled excavation and thus lacks context, both the settlement and the burial are associated to the *Cogotas* culture of the Late Bronze Age, whose most characteristic element is the type of ceramic decoration termed Boquique (Fig. S1.5A&B). This type of decoration is found in a vast number of the ceramics found(14, 15).

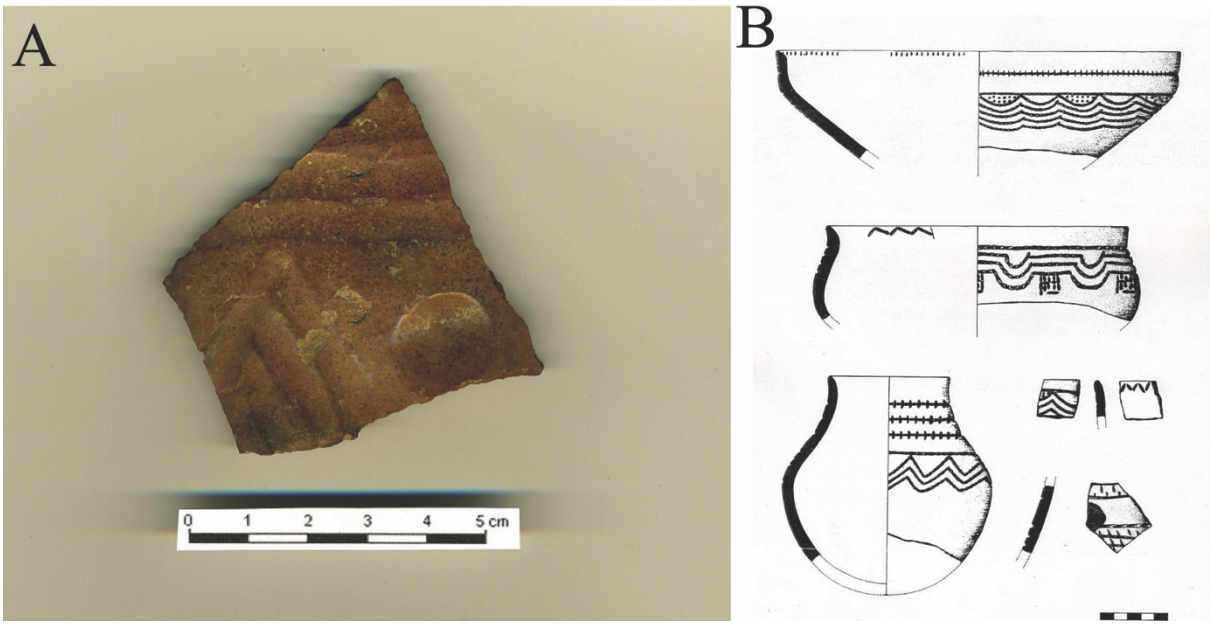


**Fig. S1.5**: **(A)** Ceramic with grooved decoration from Cueva de los Lagos. **(B)** Illustration of the Boquique ceramic decoration found at the site

### *S1.6 San Quílez*

The funerary site of San Quílez is located in San Martín Zar (Treviño County in northern Spain) at 705 m above sea level at the high end of the red river valley. Prior to its excavation in 2007, the site appeared as small natural hill, two metres high, until a road cut uncovered a few human skeletal remains together with pieces of prehistoric stone tools. Subsequent controlled excavations followed, uncovering three stratigraphic levels; 1) Superficial level: brown and greyish soils with abundant roots coming from the vegetation cover and sandy lose sediment of 15cm width at most. Only a few archaeological remains were recovered but with no associated cultural context, 2) Level 1: dark brown sediment of sandy texture with presence of limestone blocks and conglomerates that constitute an anthropic soil constructed only in the central area of the tumulus. This level contained evidence of remains within an archaeological context, 3) Level 2: soil of compact orange-brown clay. In the first layers, a few limestone blocks can be found as a continuation of the previous ones (level 1) and it is in this level where most of the skeletal material was found. Archaeological material is less frequent in deeper areas (16).

From the archaeological material recovered, the most abundant finds were the human skeletal remains: 75 lose teeth and various almost complete mandibles, a tibial fragment, one complete clavicle and a skull fragment. Most of the human remains (~75%) were found concentrated at the central and highest point of the tumulus and comprised a minimum number of individuals of eight.

The direct radiocarbon date obtained from the tooth analysed in this study (SAN216) was 5710 to 5587 years cal BP (see Table S3.2). This date is very close to the one from the nearby dolmen of La Chabola de la Hechicera (Beta 307795: 4940+30 and Beta 307796: 4980+30), which falls within the beginnings of the Basque megalithic period (and thus Iberian) placing San Quílez at the earliest phase of the Iberian megalithic.

The site of San Quílez is a secondary burial interpreted as an atypical funerary setting when compared to other sites from the region at this time, where human remains of at least eight individuals were buried at the centre of the tumulus and covered by a bed of rocks and selected blocks. (17, 18).

## S2 Sample Information and Preparation

Genomic sequence data was obtained from bone and tooth samples belonging to thirteen ancient Iberian farmers from the south and north of Spain (Table S2.1). Most samples were prepared in dedicated ancient DNA (aDNA) facilities at the Evolutionary Biology Centre in Uppsala, Sweden, except for one sample (ESP005) that was prepared at Stockholm University aDNA facilities.

**Table S2.1: Details of samples sequenced in this study including site and bone elements. Samples marked with * have been analysed for stable isotope data, samples marked with § do not include bulk nitrogen isotope data.**

| aDNA Lab code | Sample ID | Archaeological Site | Anatomical element | Reference for sequence data |
|---|---|---|---|---|
| MUR* | MZ 93-SF | Murciélagos de Zuheros, Andalusia | Bone | This study |
| C40331 | 331 | Cueva de los Cuarenta, Andalusia | Tooth | This study |
| PIR001 | P1/1988/67/1 | Priego de Córdoba, Andalusia | Tooth | This study |
| ATP2*§ | ATP2 | El Portalón, Atapuerca | Bone (femur) | Günter et al, 2015 and this study |
| ATP5*§ | ATP5 | El Portalón, Atapuerca | Bone (radius) | This study |
| ATP12*§ | ATP12-1420 | El Portalón, Atapuerca | Tooth and bone (rib) | Günter et al, 2015 and this study |
| ATP16*§ | ATP16 | El Portalón, Atapuerca | Bone (vertebrae) | Günter et al, 2015 and this study |
| ATP19*§ | ATP19 | El Portalón, Atapuerca | Bone (metacarpal) | This study |
| POR002* | ATP04 ExcW | El Portalón, Atapuerca | Bone (Tibia) | This study |
| POR003* | ATP14-545 | El Portalón, Atapuerca | Bone (Ulna) | This study |
| POR004* | ATP09-443 | El Portalón, Atapuerca | Bone (Rib) | This study |
| ESP005 | CL1 | Cueva de los Lagos, La Rioja | Tooth | This study |
| SAN216* | SQ-216 | San Quílez, Basque country | Tooth | This study |

Human samples from Andalusia (Murciélagos de Zuheros, El Pirulejo and Cueva de los Cuarenta) were collected from the Museo Histórico Municipal in Priego de Córdoba and at the Universidad de Huelva. The human remains from the site of El Portalón, San Quílez and Cueva del Lagos were collected at the Universidad de Burgos.

### *S2.1 DNA extraction and Library preparation*

All surfaces of the bone and teeth were UV irradiated (6 J/cm2 at 254 nm). The first millimetre of the bones and teeth was abraded using a Dremel™ tool and then ground into powder using a multitool drill (Dremel™) or mixer Mill (VWR STAR-BEATER). Between one hundred and two hundred milligrams of this bone/tooth powder were used for DNA extraction following a silica binding method (19). Between one and three DNA extractions were performed for each individual. All extractions were carried out in batches of eight consisting of seven samples and one extraction blank. These extraction blanks were continued throughout the whole preparation process including each step of library preparation until quantitative PCR (qPCR) and/or PCR and subsequent quantification.

Given the degraded nature of ancient DNA, we constructed DNA libraries by omitting the initial fragmentation step. Twenty microliters of extracted DNA were converted into Illumina multiplex sequencing libraries (blunt end ligation method), following (20). One to three double-stranded libraries per extract were built resulting in a total of one to nine libraries per individual.

In order to determine the optimal number of PCR cycles for library amplification qPCR was performed. Each reaction was prepared in a total volume of 25µl, containing 1µl of DNA library, 1X MaximaSYBRGreen mastermix and 200nM each of IS7 and IS8(20) reactions were set up in duplicates.

DNA libraries were enriched by amplifying four to twelve replicates with one negative PCR control per index-PCR. Library amplification were performed as in (9), using indexed primers (20) and eight to twenty cycles.

All the blanks tested throughout the process showed no presence of DNA equivalent to that of a DNA sample in neither the qPCR, Tapestation and Bionalyzer 2100 (Agilent) using the High Sensitivity DNA chip, and thus, these were not further analysed. The best libraries were selected through a DNA screening process in which ~ ten to twenty libraries were pooled at equimolar concentrations and shotgun sequenced on an Illumina HiSeq 2500 (125bp paired-end reads) or HiSeqXTen (150bp paired-end reads) at the SNP & SEQ Technology Platform at Uppsala University. From these initial results, libraries with <1% endogenous DNA and low levels of library complexity were excluded from further sequencing. Selected libraries continued to be

sequenced until saturation resulting in fifty libraries corresponding to thirteen individuals being sequenced in total.

## S3 Isotopic Analysis and Radiocarbon dates

### *S3.1 Stable Isotope Analysis*

Previous studies investigating palaeodiet during the Iberian late Neolithic-Early Bronze Age have been carried out using stable isotope analysis of bone collagen extracted from skeletal remains (summarized in (21-27). Despite the comprehensive geographic sample, these studies have demonstrated a remarkable homogeneity of stable isotope values across Iberia and a subsequent uniform interpretation that, during this period the inhabitants of Iberia consumed mainly (almost exclusively) $C_3$ terrestrial foods, with no significant intake of protein from marine or freshwater sources, despite the likely availability of these resources at many sites [there are some individuals that do show aquatic protein intake e.g.(27), but such examples are exceptions to the overall pattern of terrestrial protein diets in the Neolithic/Copper age]. Freshwater resource intake is difficult to detect using only bulk collagen carbon and nitrogen isotope data (especially when contrasting with $C_3$ terrestrial environments). Moreover, it has recently been suggested that bulk isotope values are influenced by the routing of certain amino acids that may be differentially abundant in different diets, (28). The effects of this routing on bulk isotope values (and on dietary interpretations) have yet to be fully understood or quantified. However, it has been posited that freshwater and terrestrial C3 diets can be more easily distinguished using stable carbon isotope values of amino acids in bone collagen hydrolysates(29, 30). A subsample of the individuals studied for DNA in this study underwent amino-acid stable carbon isotope analysis of bone collagen in order to determine long –term dietary preferences of these individuals. This data was supplemented by bulk $\delta^{13}C$ and $\delta^{15}N$ values provided with the radiocarbon dates of the bone collagen (Table S2.1).

### *S3.2 Sample preparation for LC-IRMS amino acid carbon isotope analysis*

Archaeological bone collagen was isolated from bone samples following a modified Longin method (31, 32). A bone chunk (approximately 200-500mg) was mechanically cleaned and abraded using a rotary hand tool (Dremel™) to remove surface dirt. The weighed chunk was demineralized in 0.5 M HCl solution at 4ºC for up to two weeks and the acid insoluble fraction was rinsed and then gelatinized at 70ºC in HCl (pH 3). The gelatin was subsequently filtered through a 5-8μm Ezee® mesh filter and lyophilized for 48 hours.

Amino acid hydrolysis, was carried out using approximately 0.5mg of bone collagen hydrolysed with 0.5ml of 6M HCl (amino acid free) in an evacuated hydrolysis tube at 110°C for 24 hours. After hydrolysis, samples were transferred to clean glass vessels and dried in a rotary vacuum

concentrator. The dried hydrolysates were frozen at -20°C until required for analysis. Prior to analysis the hydrolysates were resolved with 240µl milliQ water and 10µl of a ~50µmole solution of 2-amino isobutyric acid (Internal standard). An aliquot of the resolved stock was then diluted 1:1 with milliQ water for analysis. Each hydrolyzed collagen sample was run in duplicate on the LC-IRMS to assess the precision of the measurements.

### *S3.3 Instrumental analysis*

Separation of the amino acids in the hydrolysates and measurement of the $\delta^{13}C$ values was carried out using a Thermo Fisher LC-IRMS system consisting of a Thermo Acella LC system connected to a Thermo LC-Isolink and a Thermo Delta V Plus Mass Spectrometer. Chromatographic separation of the amino acids was achieved following methods similar to those described (33), following (34). In brief, a Primesep A column (2.1x250mm, 5um, SiELC) and a gradient elution program with three mobile phases: (A = 1L $H_2O$ + 50µl (1:50 $H_2SO_4$); B = 0.1% $H_2SO_4$ and 10mM $K_3PO_4$; C = 0.3% $H_2SO_4$) was used to separate the amino acids. Elution was achieved using similar flow rates and phase changes as those described in (33). Oxidation reagents (oxidant and acid catalyst) were the same as those described in (33). Carbon isotopic measurements were made relative to $CO_2$ reference gas pulsed into the runs at regular intervals ($\delta^{13}C_{V\text{-}PDB}$ = -0.29), which had been calibrated against USGS40 (Glutamic acid $\delta^{13}C_{V\text{-}PDB}$ = -26.39 ± 0.04‰). Amino acid peaks were manually integrated using ISODAT NT 2.0 software (Thermo Fisher) to provide a carbon isotope value for each amino acid fraction in the collagen hydrolysate (Table S3.1).

### *S3.4 Bulk Isotope Data*

Bulk isotope data was received from radiocarbon laboratories where bone samples were sent to date (BETA Analytic, Waikato) not all laboratories provided collagen quality and yield data. This data was likely produced from bone collagen extraction procedures similar to those described above and the isotope values measured using EA-IRMS.

### *S3.5 Results*

The results are summarized in Figure S3.1 and Table S3.1 below and demonstrate that the data for all individuals analysed (Table S3.1) are in agreement with previous studies. The bulk isotope data ($\delta^{13}C$ -20.1 to -18.7‰; $\delta^{15}N$ +7.6 to +11.8‰) falls within the expected range of values from previous studies, i.e. $C_3$ terrestrial diet (see (21) for a review of much of this data), and other references cited above). The amino acid stable carbon isotope data is also generally consistent with previously published European $C_3$ terrestrial data (30) (Figure S3.1). Specific aquatic dietary markers, $\Delta_{Gly\text{-}Phe}$ and $\Delta_{Val\text{-}Phe}$ spacings in this data are low (+10.5 to +15.6‰ and -0.8 to +1.6‰ respectively) also indicating a terrestrial diet (29, 30). Overall this data provides evidence that these individuals maintained a $C_3$ terrestrial diet and concurs with previous studies indicating that neither freshwater, nor marine sources of protein significantly contributed to the diet of Iberians during the Neolithic and Chalcolithic.

The individuals tested here have different genetic compositions and span over 4000 years with the sites >600km apart (north to south) and yet they have remarkably similar dietary preferences.

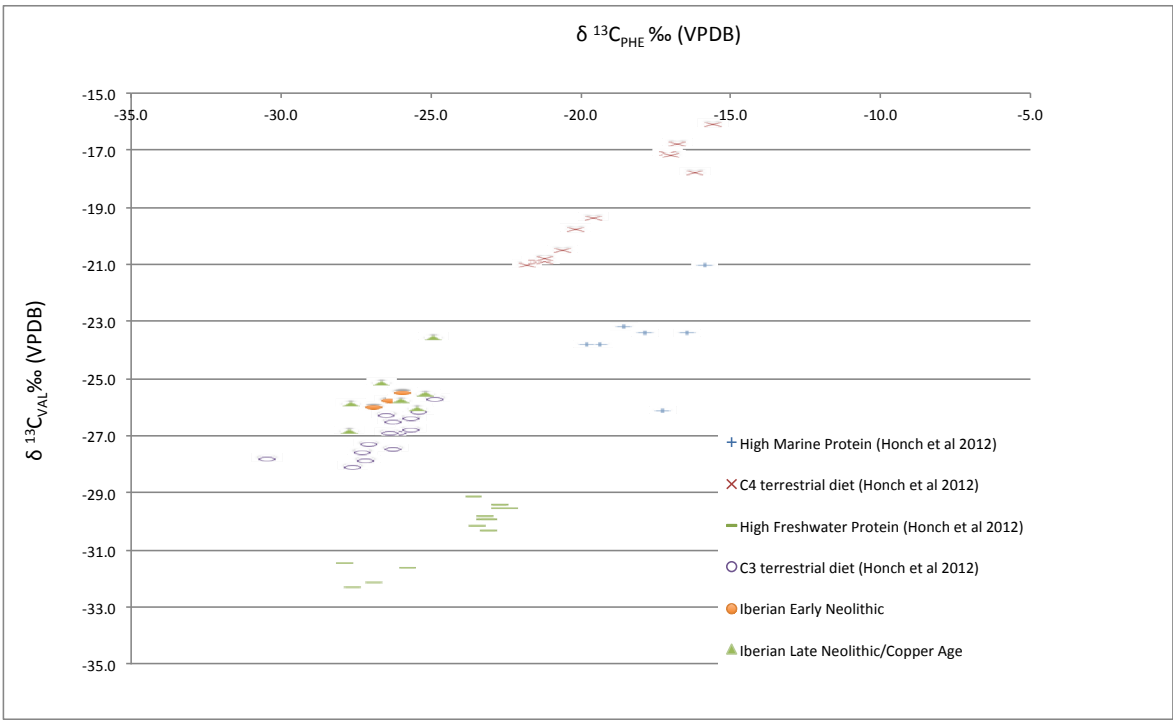


**Fig. S3.1**: Stable carbon isotope ratios of Valine vs Phenylalanine. Data from (30) is used to demonstrate known dietary regimes and where they plot in this space. Data generated in this study is plotted in two chronological groups (Early Neolithic, MUR ATP5 and ATP19; Late Neolithic/Copper Age, POR002, POR003, POR004, SAN216, ATP2, ATP12, ATP16).

**Table S3.1: Stable isotope data from bone collagen extracts from Iberian samples. Bulk collagen data ($\delta^{13}C_{COLLAGEN}$ and $\delta^{15}N_{COLLAGEN}$) was produced by radiocarbon laboratories, amino acid data was produced from hydrolysed collagen extracts in the Molecular Archaeology Laboratory, La Trobe University (from duplicate runs). Some amino acid values are not given, as data was deemed unreliable due low peak areas or co-elution with another amino acid fraction. Nitrogen and carbon isotope values are relative to AIR and VPDB scales respectively. Mass balance calculations are made using weighted averages of isotopic values of the amino acids following the amounts in collagen reported in (30).**

| SAMPLE | POR002 | | POR003 | | POR004 | | MUR | | SAN216 | | ATP2 | | ATP5 | | ATP12 | | ATP16 | | ATP19 | |
|---|---|---|---|---|---|---|---|---|---|---|---|---|---|---|---|---|---|---|---|---|
| **BULK** | | | | | | | | | | | | | | | | | | | | |
| $\delta^{13}C_{COLLAGEN}$ | -20.1 | | -19.1 | | -19 | | -19.35 | | -19.4 | | -19.2 | | -19.9 | | -18.7 | | -19 | | -18.9 | |
| $\delta^{15}N_{COLLAGEN}$ | 7.6 | | 9.9 | | 9.4 | | 9.3 | | 11.8 | | N/A | | N/A | | N/A | | N/A | | N/A | |
| **AMINO ACID** | | | | | | | | | | | | | | | | | | | | |
| $\delta^{13}C_{MASS\ BALANCE}$ | -19.4 | | -19.4 | | -19.1 | | -19.2 | | -20.3 | | -18.3 | | -19.6 | | -18.3 | | -18.3 | | -19.7 | |
| | | | | | | | | | | | | | | | | | | | | |
| | **Avg** | **S.D** | **Avg** | **S.D** | **Avg** | **S.D** | **Avg** | **S.D** | **Avg** | **S.D** | **Avg** | **S.D** | **Avg** | **S.D** | **Avg** | **S.D** | **Avg** | **S.D** | **Avg** | **S.D** |
| $\delta^{13}C_{ALA}$ | -20.1 | 1.0 | -20.9 | 0.0 | -19.7 | 0.8 | -20.2 | 0.8 | -22.9 | 0.2 | -21.5 | 0.9 | -20.8 | 0.5 | -20.2 | 0.3 | -21.2 | 0.8 | -21.0 | 0.6 |
| $\delta^{13}C_{ARG}$ | -20.6 | 1.9 | -20.9 | 0.6 | -21.8 | 2.1 | -20.5 | 1.6 | -22.1 | 0.1 | -19.3 | 0.2 | -20.5 | 1.7 | -20.0 | 0.2 | -20.0 | 0.0 | -21.2 | 0.2 |
| $\delta^{13}C_{ASX}$ | -21.1 | 0.7 | -20.6 | 0.1 | -20.0 | 0.3 | -20.9 | 0.6 | -21.2 | 0.2 | -19.5 | 0.2 | -20.9 | 0.3 | -19.7 | 0.2 | -19.3 | 0.2 | -20.9 | 0.7 |
| $\delta^{13}C_{GLX}$ | -18.1 | 1.0 | -17.9 | 0.6 | -17.0 | 0.1 | -17.5 | 0.7 | -18.3 | 0.5 | -16.7 | 0.0 | -18.2 | 0.0 | -17.0 | 0.3 | -17.1 | 0.7 | -18.5 | 0.9 |
| $\delta^{13}C_{GLY}$ | -13.5 | 0.3 | -13.2 | 0.8 | -12.0 | 0.5 | -12.5 | 1.2 | -13.8 | 0.4 | -14.4 | 0.7 | -13.3 | 0.1 | -11.5 | 0.0 | -12.0 | 1.2 | -13.9 | 0.6 |
| $\delta^{13}C_{HIS}$ | -16.6 | 0.6 | -16.8 | 0.5 | -15.4 | N/A | -19.3 | N/A | N/A | N/A | -15.2 | 0.1 | -17.8 | 1.7 | -19.0 | 0.5 | -16.9 | 0.1 | N/A | N/A |
| $\delta^{13}C_{HYLYS}$ | -21.4 | 0.2 | -21.8 | 0.7 | -23.0 | 0.8 | -21.9 | 1.1 | -22.5 | 0.2 | -19.6 | 0.5 | -21.0 | 1.0 | -20.2 | 0.3 | -19.9 | 0.3 | -23.7 | 2.1 |
| $\delta^{13}C_{HYP}$ | -20.2 | 0.7 | -19.6 | 0.0 | -19.5 | 0.4 | -20.1 | 0.7 | -20.1 | 0.1 | -17.6 | 0.4 | -20.3 | 0.2 | -19.2 | 0.3 | -18.9 | 0.5 | -19.7 | 0.3 |
| $\delta^{13}C_{ILE}$ | -23.4 | 2.6 | -23.0 | 0.5 | -24.2 | 2.0 | -23.4 | 3.0 | -25.7 | 1.2 | -21.6 | 0.2 | -22.9 | 2.7 | -22.2 | 0.1 | -23.2 | 0.6 | -23.6 | 0.7 |
| $\delta^{13}C_{LEU}$ | -29.5 | 2.1 | -29.1 | 0.4 | -29.8 | 1.5 | -29.0 | 1.4 | -30.0 | 0.4 | -28.1 | 0.5 | -29.3 | 1.2 | -28.8 | 0.1 | -28.7 | 0.4 | -29.6 | 0.8 |
| $\delta^{13}C_{LYS}$ | -21.5 | 1.0 | -21.4 | 0.6 | -22.4 | 1.6 | -21.3 | 1.6 | -22.5 | 0.0 | -19.7 | 0.4 | -21.6 | 1.4 | -20.4 | 0.2 | -20.8 | 0.3 | -21.6 | 0.3 |
| $\delta^{13}C_{MET}$ | -27.3 | 0.1 | -28.0 | 1.7 | -29.7 | 1.0 | -28.9 | 1.5 | -28.1 | 1.9 | 1.1 | 0.0 | -28.2 | 1.9 | -30.2 | 0.2 | -27.8 | 0.3 | -27.8 | 0.8 |
| $\delta^{13}C_{PHE}$ | -26.0 | 1.6 | -26.7 | 0.7 | -27.7 | 2.1 | -26.0 | 2.0 | -27.7 | 0.3 | -24.9 | 0.2 | -26.4 | 2.0 | -25.2 | 0.6 | -25.5 | 0.4 | -26.9 | 0.6 |
| $\delta^{13}C_{PRO}$ | -20.3 | 0.8 | -20.2 | 0.6 | -20.1 | 0.2 | -20.5 | 1.0 | -20.6 | 0.1 | -16.9 | 0.3 | -20.8 | 0.3 | -18.2 | 0.4 | -17.2 | 0.1 | -20.6 | 0.8 |
| $\delta^{13}C_{SER}$ | -14.1 | 0.1 | -14.2 | 0.9 | -13.4 | 0.5 | -12.7 | 1.7 | -16.7 | 0.1 | -15.2 | 4.4 | -14.4 | 0.9 | -13.2 | 2.9 | -11.9 | 1.4 | -14.6 | 0.8 |
| $\delta^{13}C_{THR}$ | -9.3 | 0.2 | -11.0 | 1.5 | -9.8 | 1.1 | -10.2 | 0.6 | -11.6 | 0.0 | -10.3 | 2.2 | -10.7 | 0.5 | -10.8 | 0.5 | -11.2 | 2.9 | -11.1 | 1.2 |
| $\delta^{13}C_{TYR}$ | -23.3 | 1.4 | -24.9 | 0.9 | -23.9 | N/A | -26.4 | N/A | N/A | N/A | -24.6 | 0.3 | -24.1 | 1.0 | -21.8 | 0.2 | -24.2 | 0.9 | N/A | N/A |
| $\delta^{13}C_{VAL}$ | -26.0 | 1.2 | -25.4 | 0.4 | -26.1 | 1.0 | -25.7 | 1.4 | -27.1 | 0.4 | -23.8 | 0.3 | -26.0 | 0.4 | -25.7 | 0.1 | -26.3 | 0.1 | -26.2 | 0.1 |
| | | | | | | | | | | | | | | | | | | | | |
| $\delta^{13}C_{GLY}$-$\delta^{13}C_{PHE}$ | 12.5 | | 13.4 | | 15.6 | | 13.4 | | 13.9 | | 10.5 | | 13.1 | | 13.7 | | 13.5 | | 13.0 | |
| $\delta^{13}C_{VAL}$-$\delta^{13}C_{PHE}$ | 0.0 | | 1.3 | | 1.6 | | 0.3 | | 0.7 | | 1.2 | | 0.4 | | -0.5 | | -0.8 | | 0.7 | |

### *S3.6 Radiocarbon dates*

Nine new human remains were directly radiocarbon dated in this study using accelerator mass spectrometry (AMS) at Beta Analytic Inc. (Miami, Florida) and the Waikato Radiocarbon Dating Laboratory (New Zealand). These nine dates together with four previously published dates (9) were calibrated to years cal BP using Oxcal v4.3.2 software based on the IntCal13 atmospheric curve(35) (Table S3.2). Only two samples were not radiocarbon dated and these belong to well contextualised Bronze Age samples from the sites of El Pirulejo(4) and Cueva de los Lagos(15). Overall, the radiocarbon dates cover a time period from the early Neolithic to the Bronze Age (Figure S3.2)

**Table S3.2: Details of samples radiocarbon dated and calibrated in this study.**

| Sample ID | Laboratory | C14 lab code | Site | Result BP/Conventional Age | 2 Sigma Calibration Cal BP | Reference |
|---|---|---|---|---|---|---|
| MUR | Waikato-New Zealand | wk-40844 | Murciélagos de Zuheros, Andalusia | 6226 +/- 20 BP | 7245 to 7025 | This study |
| C40331 | Beta Analytic-USA | Beta-424648 | Cueva de los Cuarenta, Andalusia | 4900 +/- 30 BP | 5710 to 5587 | This study |
| ATP2 | Beta Analytic-USA | Beta-386394 | El Portalón, Atapuerca | 4210 +/- 30 BP | 4849 to 4628 | Günter et al, 2015 |
| ATP5 | Beta Analytic-USA | Beta-368283 | El Portalón, Atapuerca | 6170 +/- 30 BP | 7165 to 6980 | This study |
| ATP9 | Beta Analytic-USA | Beta-386395 | El Portalón, Atapuerca | 3390 +/- 30 BP | 3700 to 3568 | Günter et al, 2015 |
| ATP12 | Beta Analytic-USA | Beta-368295 | El Portalón, Atapuerca | 4300 +/- 30 BP | 4960 to 4829 | Günter et al, 2015 |
| ATP16 | Beta Analytic-USA | Beta-368289 | El Portalón, Atapuerca | 4400 +/- 30 BP | 5211 to 4866 | Günter et al, 2015 |
| ATP19 | Beta Analytic-USA | Beta-368292 | El Portalón, Atapuerca | 6170 +/- 30 BP | 7165 to 6980 | This study |
| POR002 | Beta Analytic-USA | Beta-424645 | El Portalón, Atapuerca | 4450 +/- 30 BP | 5285 to 4894 | This study |
| POR003 | Beta Analytic-USA | Beta-424646 | El Portalón, Atapuerca | 4680 +/- 30 BP | 5572 to 5319 | This study |
| POR004 | Beta Analytic-USA | Beta-424647 | El Portalón, Atapuerca | 4390 +/- 30 BP | 5041 to 4867 | This study |
| SAN216 | Beta Analytic-USA | Beta-424654 | San Quílez, Basque country | 4940 +/- 30 BP | 5726 to 5603 | This study |

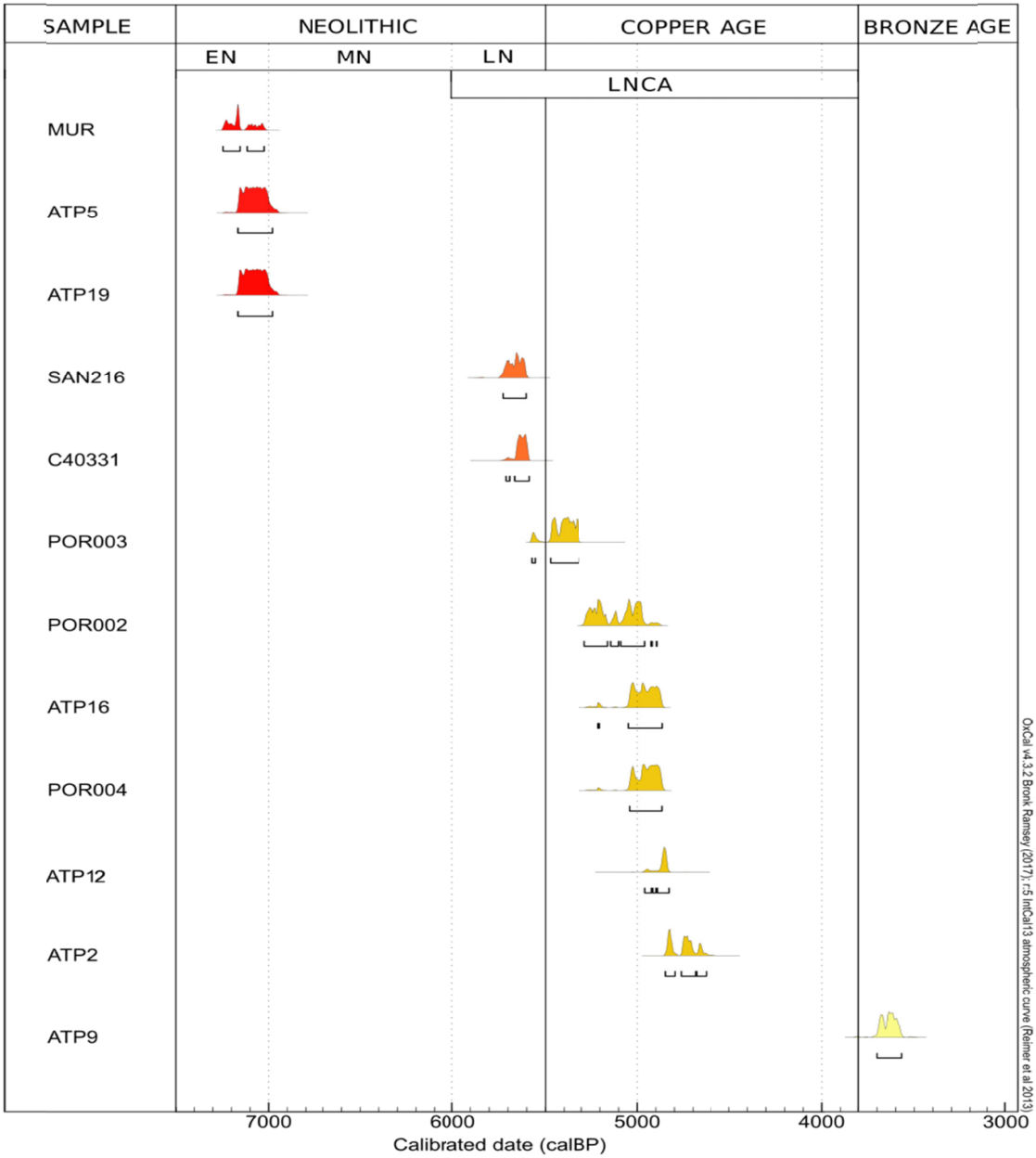


**Fig. S3.2**: Composite chronology, based on calibrated radiocarbon dates, for samples in this study, including approximate dates of cultural periods within Iberia. Abbreviations: EN - Early Neolithic (~7500-6700 cal BP), MN - Middle Neolithic (~6700-6000 cal BP), LN - Late Neolithic (~6000-5500), LNCA- Late Neolithic/Copper Age (~6000-4000 cal BP), BA – Bronze Age (~4000-2900 cal BP).

**S4 NGS data processing and estimation of contamination**

Overlapping paired-end reads were merged requiring an overlap of at least 11 bases (using *MergeReadsFastQ_cc.py*, (36). After trimming of remaining adapters, the fragments were mapped to the human reference genome using *bwa aln* (37) with the non-default parameters -l 16500 -n 0.01 and -o 2. Consensus sequences were called for fragments mapping to identical coordinates as they likely represent PCR duplicates (using a modified *FilterUniqSAMCons_cc.py*, (36, 38). Only fragments with at least 90% identity to the reference genome, a minimum length of 35bp and mapping qualities of 30 or higher were used for subsequent analysis. Different libraries and sequencing runs for the same individual were merged into one final BAM file using *samtools* v0.1.19(39). Biological sex was assigned by comparing the numbers of fragments mapping to the sex chromosomes (Table S4.1) (40).

Two approaches were used to estimate the level of contamination per sample. First, the proportion of non-consensus reads at sites showing nearly private alleles in the mitochondrial consensus of each sample (less than 5% frequency in a diverse set of 311 modern mitochondrial sequences, (41) was used to obtain an estimate for mitochondrial contamination. This analysis was restricted to sites with at least 10x coverage, a minimum base quality of 30, and transition sites with a G or C in the consensus were excluded to avoid biases due to post-mortem damage. Second, heterozygous transversion sites on the X chromosome of male samples were used to obtain an estimate of nuclear contamination for those samples using the method described in (42) which was implemented in *ANGSD* (43). This analysis excluded the pseudoautosomal region of the X chromosome and a minimum base and mapping quality threshold of 30 was applied while now coverage filter was used. We report the result of *ANGSD*'s method 1 in Table S4.1.

Two samples (ATP019 and POR003) showed high levels of mitochondrial contamination (>15%). Consequently, we used *PMDTOOLS* (44) and different cut-offs to restrict downstream analysis to authentic fragments. We re-estimated the mitochondrial contamination after filtering until a contamination <5% was reached or not enough data was left to obtain an estimate (Table S4.1). In order to investigate whether this filtering would affect our results, we used one sample (esp005) with low estimates of contamination (<3.5%), filtered it up to a PMD score of 11 and compared its location in the PC1-PC2 space to the full data for esp005. While reducing the amount of data adds noise to the precise position of esp005, we do not observe a trend biasing the signal into any specific direction (Fig S4.2).

**Table S4.1: Sequencing statistics and contamination rates for newly generated sequence data**

| Individual | Site/Geography | Nuclear cov | mt cov | Sex | mt cont. | X cont. | mt HG | Y HG | C14 Cal BP | Classification |
|---|---|---|---|---|---|---|---|---|---|---|
| atp002[&] | El Portalón/North | 8.71 | 703.36 | XY | 0.10 [0-0.22] | 0.0255 | U5b3 | H2-P96 | 4849-4628 | Copper Age |
| atp005 | El Portalón/North | 0.08 | 19.71 | XY | 4.11 [1.13-7.10] | 0.0025 | J2b1a | * | 7165-6980 | Early Neolithic |
| atp016[&] | El Portalón/North | 12.98 | 692.91 | XX | 1.59 [1.16-2.02] | - | X2c2 | - | 5211-4866 | Copper Age |
| atp019 | El Portalón/North | 2.88 | 223.40 | | | | | | | |
| atp019[$] | El Portalón/North | 0.03 | 3.54 | XX | - | - | N1 | - | 7165-6980 | Early Neolithic |
| atp12-1420[&] | El Portalón/North | 2.43 | 347.3 | XY | 0.36 [0-0.78] | 0.0138 | H3c | I2-M223 | 4960-4829 | Copper Age |
| c40331 | Cueva de los Cuarenta/South | 0.28 | 167.53 | XY | 3.12 [1.38-4.85] | 0.0147 | HV0a | I2-Z161 | 5710-5587 | Late Neolithic |
| esp005 | Cueva de los lagos/South | 2.36 | 480.40 | XY | 1.31 [0.78-1.84] | 0.0334 | K1a | R1b-DF27 | Not C14 | Bronze Age |
| mur | Cueva de los Murciélagos/South | 3.33 | 595.62 | XY | 1.84 [1.46-2.22] | 0.0222 | J1c1b1 | G2a2-L1259 | 7245-7025 | Early Neolithic |
| pir001 | El Pirulejo/South | 0.21 | 214.27 | XY | 0.77 [0.16-1.38] | 0.0105 | K1a13 | R1b-M269 | Not C14 | Bronze Age |
| por002 | El Portalón/North | 0.81 | 104.39 | XY | 2.14 [0.99-3.29] | 0.05 | K1a2b | I2-M423 | 5285-4894 | Copper Age |
| por003 | El Portalón/North | 0.22 | 68.84 | | 27.69 [22.83-32.56] | | | | | |
| por003[#] | El Portalón/North | 0.02 | 11.37 | XY | 0.0 [0.0-7.39] | * | J1c1 | * | 5572-5319 | Copper Age |
| por004 | El Portalón/North | 0.12 | 19.33 | XY | 0 [0-5.82] | 0.0045 | K1a | I2-M436 | 5041-4867 | Copper Age |
| san216 | San Quílez/North | 0.19 | 29.49 | XY | 5.0 [1.10-8.90] | 0.0083 | X2b | * | 5726-5603 | Late Neolithic |

[$] PMD filtered with a score of 11. [#] PMD filtered with a score of 6. [&] additional data for individuals published in Günther et al 2015 (11). HG: Haplogroup. Cont.: contamination. *: not enough data

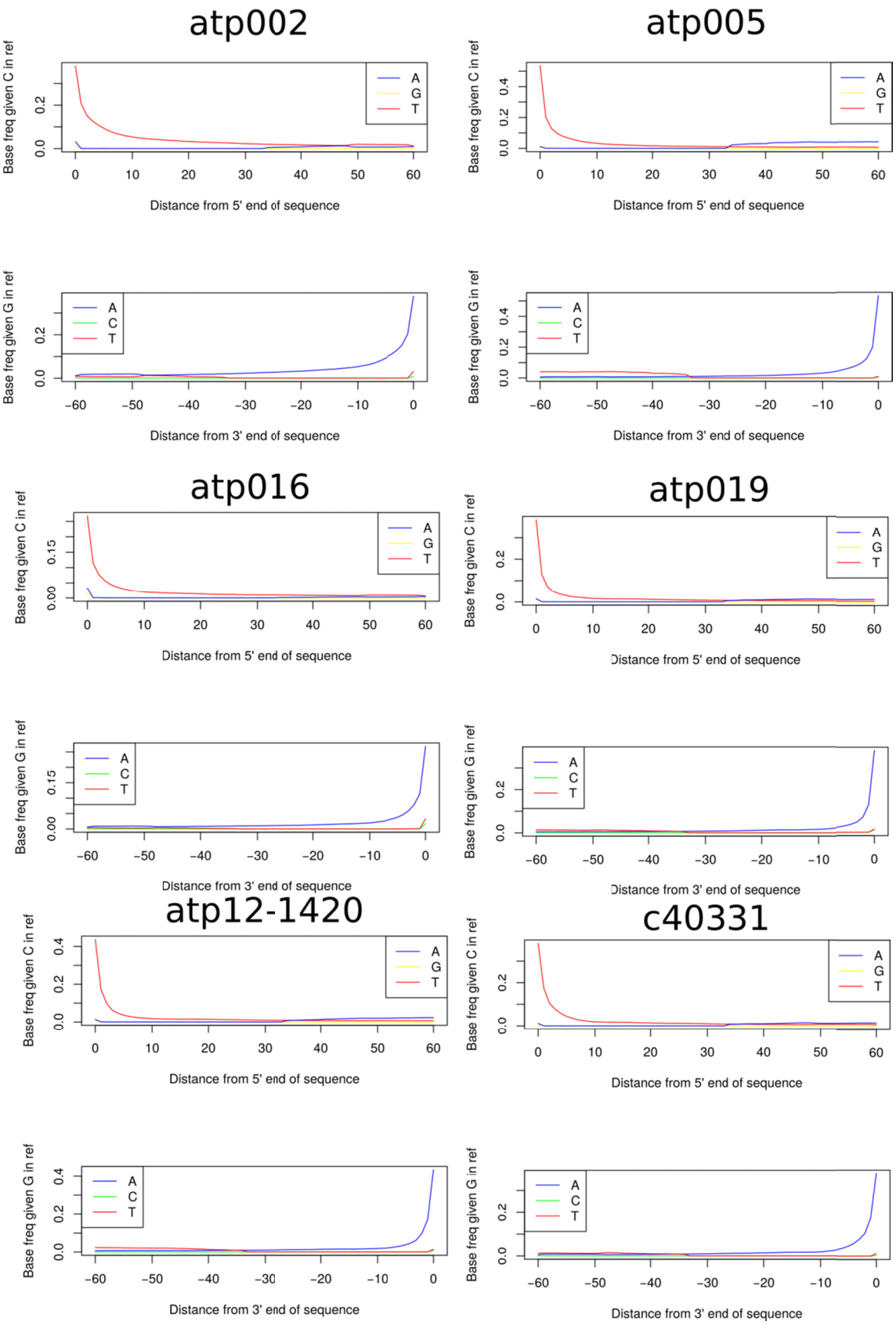
atp002
Base freq given C in ref
Base freq given G in ref
Distance from 5' end of sequence
Distance from 3' end of sequence
A
G
C
T
atp005
atp016
atp019
atp12-1420
c40331

## esp005

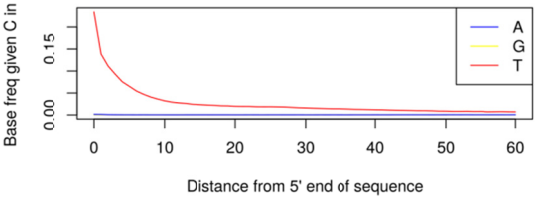


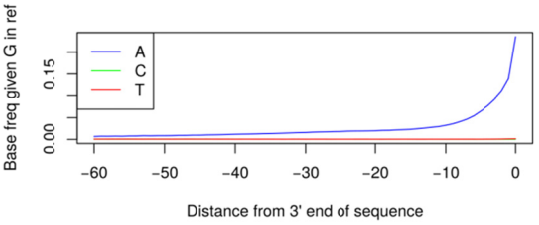


## mur

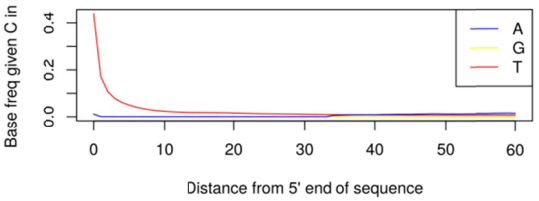


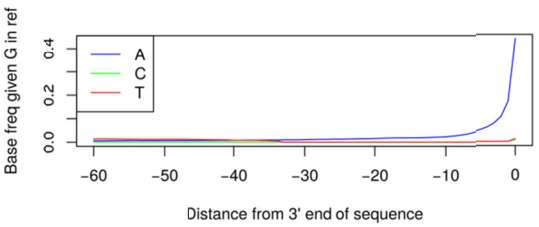


## pir001

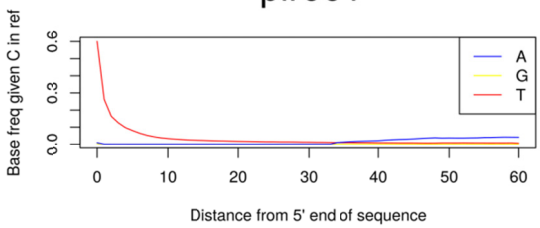


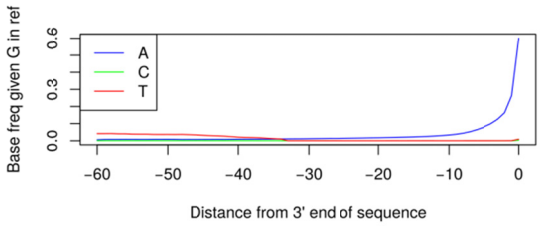


## por002

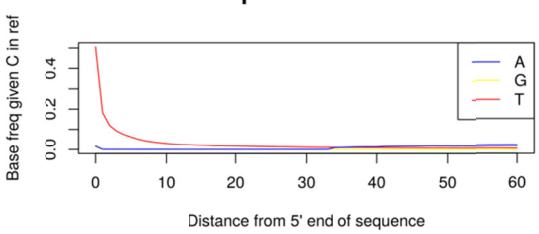


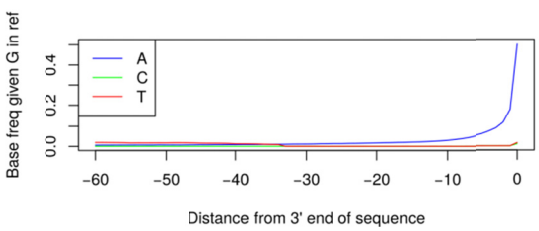


## por003

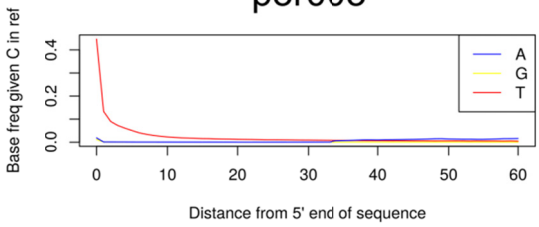


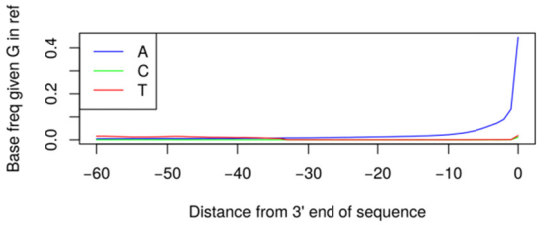


## por004

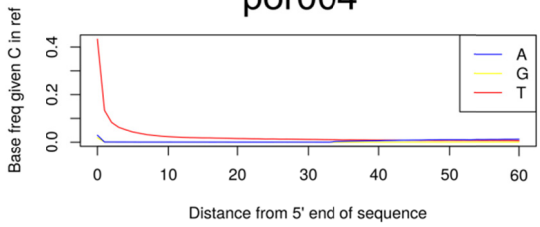


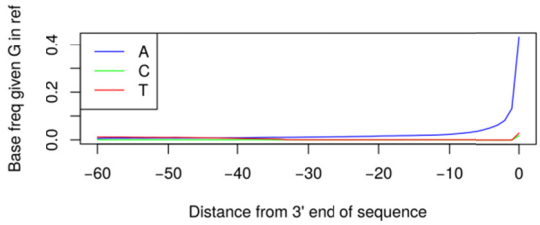

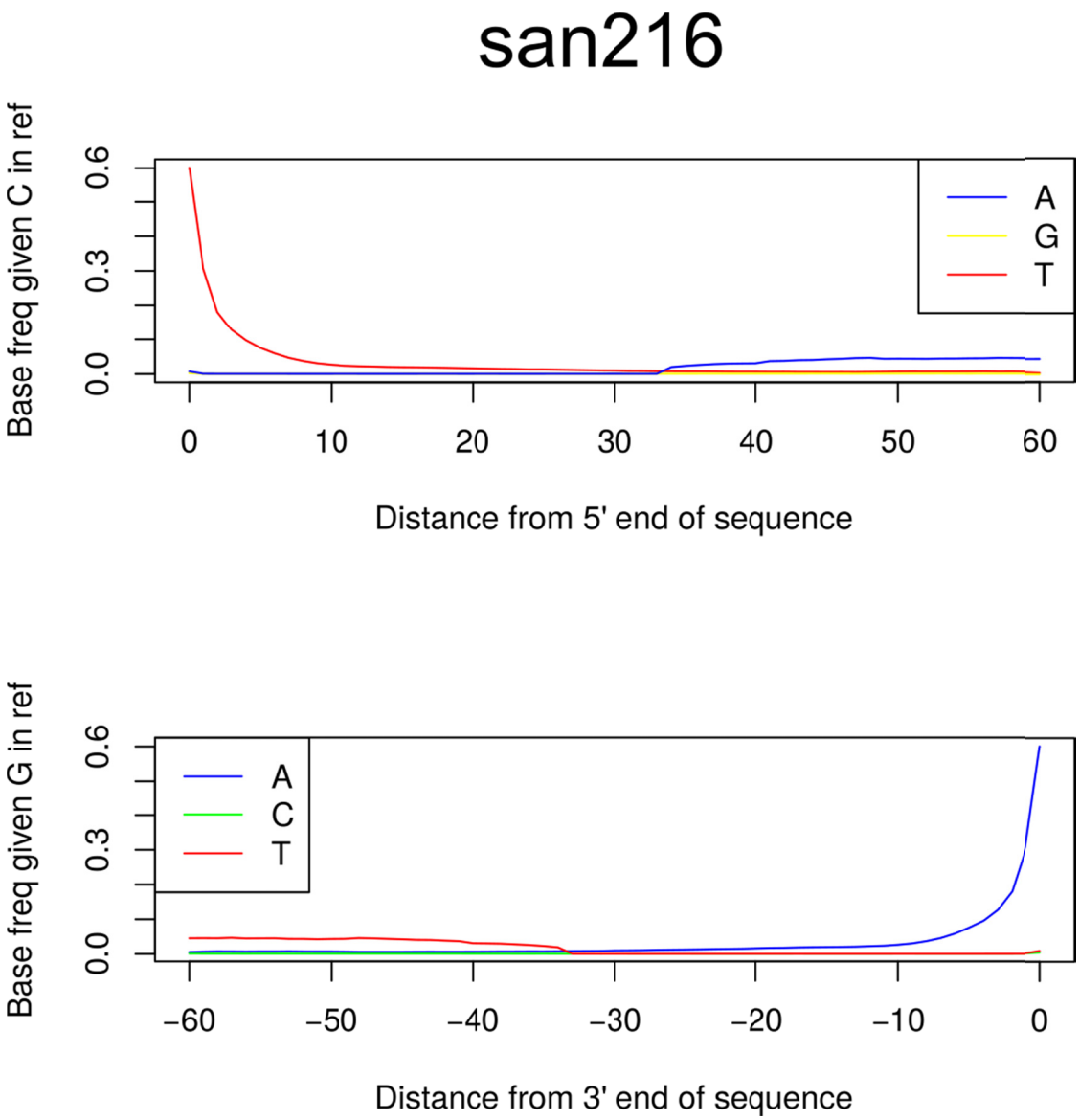


**Fig. S4.1**: Deamination patterns, characteristic of ancient DNA, of the 13 samples sequenced, showing an increase in C >T misincorporations due to cytosine deamination at the 5′-end of DNA reads and the equivalent increase of G > A misincorporations at the 3′-end.

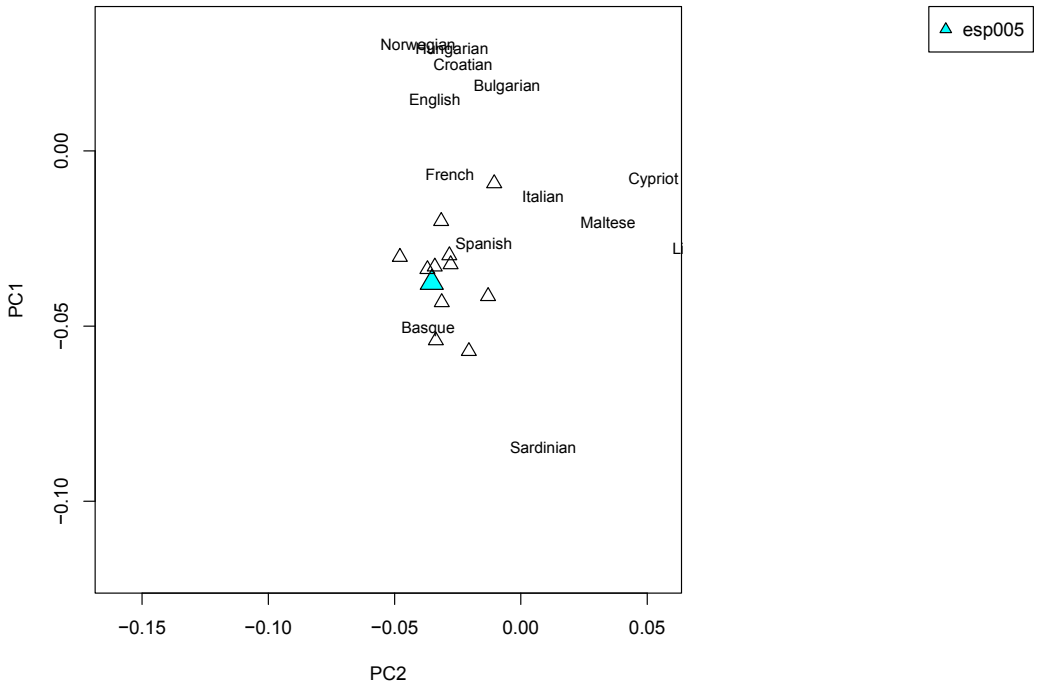


**Fig S4.2**: PC1-PC2 plot for esp005 individual (solid, big triangle) together with varying degrees of PMD score filtering (up to 11, smaller triangles). Increasing levels of transparency correspond to higher PMD score cut-offs.

## S5 Population Genetic Analysis

### *S5.1 Uniparental haplotyping*

Mitochondrial consensus sequences were called using *samtools mpileup* and *vcfutils.pl* (39) applying minimum mapping and base qualities of 30. *HAPLOFIND* (45) was then used to infer the most likely mitochondrial haplogroup. Y chromosomal haplogroups were assigned by investigating up to 732 haplotype-informative single base substitutions obtained from Phylotree (version from 2016-03-09, (46). s*amtools* v1.3 *mpileup* (39) was used to obtain all reads mapping to the corresponding positions with mapping quality of at least 30. Haplotypes were called if at least three derived alleles (minimum base quality 30) support an unambiguous path to a certain classification. Sites presenting more than one allele were not taken into account for the classification. Derived sites for all samples are shown in Dataset S1 excluding sites that did not fit a single path to the most likely haplogroup as they might represent sequencing errors, strand misidentification or contamination.

### *S5.2 Merging with other data sets*

To analyze the newly sequenced samples in context of modern and prehistoric European variation, we merged them with published data from ancient individuals (see Table S5.1) as well as 203 modern populations from the Human Origins panel (47, 48). The samples were merged for three different SNP panels: the Human Origins array (47, 48), 1.9 million transversions with minor allele frequencies of 10% or more in 1000

genomes Yorubans (9, 49) and 1.2 million SNPs used in aDNA in-solution capture procedures(50). The merged data set contained all ancient individuals as pseudo-haploids. For each SNP site a single read was randomly drawn (minimum mapping and base quality of 30) and if the allele on that read corresponded to one of the two known alleles, it was assumed as the allele carried by the ancient individual. Transitions were coded as missing data to exclude potential post-mortem damage.

### *S5.3 Principal component analysis*

For each ancient individual, a principal component analysis based on all overlapping SNPs with the Human Origins data set was conducted using *smartpca* v10210(51). Procrustes analysis (52, 53) implemented in the GNU R vegan package was then used to project each individual's coordinates in the PC1-PC2 space onto a PCA of the modern Human Origins populations using all SNP sites. The full PCA of all ancient European and Anatolian samples together with modern European populations is shown in Dataset S2, Figure 1B shows parts of this plot. Figure S5.1 shows a PCA of the ancient samples together with modern Europeans and North Africans. None of the samples exhibits affinities with the modern North African populations.

The 26 modern day populations from the Human Origins data set used here are: Adygei, Basque_French, Basque_Spanish, Bulgarian, Croatian, Cypriot, Druze, English_Cornwall_GBR, English_Kent_GBR, Finnish_FIN, French, French_South, Hungarian_Coriell, Hungarian_Metspalu, Italian_Bergamo, Italian_EastSicilian, Italian_South, Italian_Tuscan, Italian_WestSicilian, Libyan_Jew, Lithuanian, Maltese, Norwegian, Russian, Sardinian, Spanish_IBS.

**Table S5.1: Ancient samples used in this study and their assignment to groups for population-based analyses. Samples belonging to "Other" were only used for unsupervised *ADMIXTURE*.**

| Group | Sample ID | Reference |
|---|---|---|
| Anatolia_Neolithic | Bar31 | Hofmanova2016 |
| Anatolia_Neolithic | Bar8 | Hofmanova2016 |
| Anatolia_Neolithic | I0707 | Mathieson2015 |
| Anatolia_Neolithic | I0708 | Mathieson2015 |
| Anatolia_Neolithic | I0709 | Mathieson2015 |
| Anatolia_Neolithic | I0723 | Mathieson2015 |
| Anatolia_Neolithic | I0724 | Mathieson2015 |
| Anatolia_Neolithic | I0726 | Mathieson2015 |
| Anatolia_Neolithic | I0727 | Mathieson2015 |
| Anatolia_Neolithic | I0736 | Mathieson2015 |
| Anatolia_Neolithic | I0744 | Mathieson2015 |
| Anatolia_Neolithic | I0745 | Mathieson2015 |
| Anatolia_Neolithic | I0746 | Mathieson2015 |
| Anatolia_Neolithic | I1096 | Mathieson2015 |
| Anatolia_Neolithic | I1097 | Mathieson2015 |
| Anatolia_Neolithic | I1098 | Mathieson2015 |
| Anatolia_Neolithic | I1099 | Mathieson2015 |
| Anatolia_Neolithic | I1100 | Mathieson2015 |
| Anatolia_Neolithic | I1101 | Mathieson2015 |
| Anatolia_Neolithic | I1102 | Mathieson2015 |
| Anatolia_Neolithic | I1103 | Mathieson2015 |
| Anatolia_Neolithic | I1579 | Mathieson2015 |
| Anatolia_Neolithic | I1580 | Mathieson2015 |
| Anatolia_Neolithic | I1581 | Mathieson2015 |
| Anatolia_Neolithic | I1583 | Mathieson2015 |
| Anatolia_Neolithic | I1585 | Mathieson2015 |
| Central_BB | I0060 | Haak2015,Mathieson2015 |
| Central_BB | I0108 | Haak2015,Mathieson2015 |
| Central_BB | I0111 | Haak2015,Mathieson2015 |
| Central_BB | I0112 | Haak2015,Mathieson2015 |
| Central_BB | I0113 | Haak2015,Mathieson2015 |
| Central_BB | I0805 | Haak2015,Mathieson2015 |
| Central_BB | I0806 | Haak2015,Mathieson2015 |
| Central_BB | I1546 | Haak2015,Mathieson2015 |
| Central_BB | I1549 | Haak2015,Mathieson2015 |
| Central_BB | RISE559 | Allentoft2015 |
| Central_BB | RISE560 | Allentoft2015 |
| Central_BB | RISE562 | Allentoft2015 |
| Central_BB | RISE563 | Allentoft2015 |
| Central_BB | RISE564 | Allentoft2015 |
| Central_BB | RISE566 | Allentoft2015 |
| Central_BB | RISE568 | Allentoft2015 |
| Central_BB | RISE569 | Allentoft2015 |
| Central_Unetice | I0047 | Haak2015,Mathieson2015 |
| Central_CWC | I0049 | Haak2015,Mathieson2015 |
| Central_CWC | I0103 | Haak2015,Mathieson2015 |
| Central_CWC | I0104 | Haak2015,Mathieson2015 |
| Central_CWC | I0106 | Haak2015,Mathieson2015 |
| Central_Unetice | I0115 | Haak2015,Mathieson2015 |
| Central_Unetice | I0116 | Haak2015,Mathieson2015 |
| Central_Unetice | I0117 | Haak2015,Mathieson2015 |
| Central_LNBA | I0118 | Haak2015,Mathieson2015 |
| Central_Unetice | I0164 | Haak2015,Mathieson2015 |
| Central_Unetice | I0803 | Haak2015,Mathieson2015 |
| Central_Unetice | RISE109 | Allentoft2015 |

| | | |
|---|---|---|
| Central_Unetice | RISE150 | Allentoft2015 |
| Central_Unetice | RISE154 | Allentoft2015 |
| Central_Unetice | RISE577 | Allentoft2015 |
| Central_Unetice | RISE586 | Allentoft2015 |
| Central_CWC | I1532 | Haak2015,Mathieson2015 |
| Central_CWC | I1534 | Haak2015,Mathieson2015 |
| Central_CWC | I1536 | Haak2015,Mathieson2015 |
| Central_CWC | I1538 | Haak2015,Mathieson2015 |
| Central_CWC | I1539 | Haak2015,Mathieson2015 |
| Central_CWC | I1540 | Haak2015,Mathieson2015 |
| Central_CWC | I1542 | Haak2015,Mathieson2015 |
| Central_CWC | I1544 | Haak2015,Mathieson2015 |
| Central_CWC | RISE431 | Allentoft2015 |
| Central_CWC | RISE434 | Allentoft2015 |
| Central_CWC | RISE435 | Allentoft2015 |
| Central_CWC | RISE436 | Allentoft2015 |
| Central_CWC | RISE446 | Allentoft2015 |
| Central_MN | I0172 | Haak2015,Mathieson2015 |
| Central_MN | I0551 | Haak2015,Mathieson2015 |
| Central_MN | I0559 | Haak2015,Mathieson2015 |
| Central_MN | I0560 | Haak2015,Mathieson2015 |
| Central_MN | I0807 | Haak2015,Mathieson2015 |
| Central_MN | I1497 | Haak2015,Mathieson2015 |
| Central_CA | Iceman | Keller2012 |
| Central_CA | RISE486 | Allentoft2015 |
| Central_CA | RISE487 | Allentoft2015 |
| Central_CA | RISE489 | Allentoft2015 |
| Caucasus_HG | Kotias | Jones2015 |
| Caucasus_HG | Satsurblia | Jones2015 |
| EHG | I0061 | Haak2015,Mathieson2015 |
| EHG | I0124 | Haak2015,Mathieson2015 |
| EHG | I0211 | Haak2015,Mathieson2015 |
| Hungary_BA | I1502 | Gamba2014,Haak2015,Mathieson2015 |
| Hungary_BA | I1504 | Gamba2014,Haak2015,Mathieson2015 |
| Hungary_BA | RISE247 | Allentoft2015 |
| Hungary_BA | RISE254 | Allentoft2015 |
| Hungary_BA | RISE349 | Allentoft2015 |
| Hungary_BA | RISE371 | Allentoft2015 |
| Hungary_BA | RISE373 | Allentoft2015 |
| Hungary_BA | RISE374 | Allentoft2015 |
| Hungary_BA | RISE479 | Allentoft2015 |
| Hungary_BA | RISE480 | Allentoft2015 |
| Hungary_BA | RISE483 | Allentoft2015 |
| Hungary_BA | RISE484 | Allentoft2015 |
| Hungary_EN | I0174 | Gamba2014,Haak2015,Mathieson2015 |
| Hungary_EN | I0176 | Gamba2014,Haak2015,Mathieson2015 |
| Hungary_EN | I1495 | Gamba2014,Haak2015,Mathieson2015 |
| Hungary_EN | I1496 | Gamba2014,Haak2015,Mathieson2015 |
| Hungary_EN | I1498 | Gamba2014,Haak2015,Mathieson2015 |
| Hungary_EN | I1499 | Gamba2014,Haak2015,Mathieson2015 |
| Hungary_EN | I1500 | Gamba2014,Haak2015,Mathieson2015 |
| Hungary_EN | I1505 | Gamba2014,Haak2015,Mathieson2015 |
| Hungary_EN | I1506 | Gamba2014,Haak2015,Mathieson2015 |
| Hungary_EN | I1508 | Gamba2014,Haak2015,Mathieson2015 |
| IberiaNorth_BA | ATP9 | Gunther2015 |
| IberiaNorth_BA | ESP005 | this study |
| IberiaSouth_BA | PIR001 | this study |
| IberiaNorth_LNCA | ATP002 | this study, Gunther2015 |
| IberiaNorth_LNCA | ATP016 | this study, Gunther2015 |

| | | |
|---|---|---|
| IberiaNorth_LNCA | ATP12 | this study, Gunther2015 |
| IberiaNorth_LNCA | I0581 | Haak2015,Mathieson2015 |
| IberiaNorth_LNCA | I1271 | Haak2015,Mathieson2015 |
| IberiaNorth_LNCA | I1272 | Haak2015,Mathieson2015 |
| IberiaNorth_LNCA | I1276 | Haak2015,Mathieson2015 |
| IberiaNorth_LNCA | I1277 | Haak2015,Mathieson2015 |
| IberiaNorth_LNCA | I1280 | Haak2015,Mathieson2015 |
| IberiaNorth_LNCA | I1281 | Haak2015,Mathieson2015 |
| IberiaNorth_LNCA | I1282 | Haak2015,Mathieson2015 |
| IberiaNorth_LNCA | I1284 | Haak2015,Mathieson2015 |
| IberiaNorth_LNCA | I1300 | Haak2015,Mathieson2015 |
| IberiaNorth_LNCA | I1303 | Haak2015,Mathieson2015 |
| IberiaNorth_LNCA | I1314 | Haak2015,Mathieson2015 |
| IberiaNorth_LNCA | POR002 | this study |
| IberiaNorth_LNCA | POR003_pmd | this study |
| IberiaNorth_LNCA | POR004 | this study |
| IberiaNorth_EN | ATP005 | this study |
| IberiaNorth_EN | ATP019_pmd | this study |
| IberiaNorth_EN | CB13 | Olade2015 |
| IberiaNorth_EN | I0409 | Haak2015,Mathieson2015 |
| IberiaNorth_EN | I0410 | Haak2015,Mathieson2015 |
| IberiaNorth_EN | I0412 | Haak2015,Mathieson2015 |
| IberiaNorth_EN | I0413 | Haak2015,Mathieson2015 |
| IberiaSouth_EN | MUR | this study |
| IberiaSouth_MN | C40331 | this study |
| IberiaNorth_MN | I0405 | Haak2015,Mathieson2015 |
| IberiaNorth_MN | I0406 | Haak2015,Mathieson2015 |
| IberiaNorth_MN | I0407 | Haak2015,Mathieson2015 |
| IberiaNorth_MN | I0408 | Haak2015,Mathieson2015 |
| IberiaNorth_MN | SAN216 | this study |
| IberiaSouthWest_MN | LC41 | Martiniano2017 |
| IberiaSouthWest_MN | LC42 | Martiniano2017 |
| IberiaSouthWest_MN | LC44 | Martiniano2017 |
| IberiaSouthWest_MN | LC45 | Martiniano2017 |
| IberiaSouthWest_LNCA | CA117B | Martiniano2017 |
| IberiaSouthWest_LNCA | CA122A | Martiniano2017 |
| IberiaSouthWest_LNCA | CM364 | Martiniano2017 |
| IberiaSouthWest_LNCA | CM9B | Martiniano2017 |
| IberiaSouthWest_LNCA | DA96B | Martiniano2017 |
| IberiaSouthWest_LNCA | MC337A | Martiniano2017 |
| IberiaSouthWest_BA | MG104 | Martiniano2017 |
| IberiaSouthWest_BA | TV32032 | Martiniano2017 |
| IberiaSouthWest_BA | TV3831 | Martiniano2017 |
| IberiaSouthWest_BA | VO10207 | Martiniano2017 |
| Ireland_MN | Ballynahatty | Cassidy2016 |
| Anatolia_Neolithic | Klei10 | Hofmanova2016 |
| Anatolia_Neolithic | Kumtepe006 | Omrak2016 |
| Central_LBK_EN | I0022 | Mathieson2015,Lazaridis2016 |
| Central_LBK_EN | I0025 | Mathieson2015,Lazaridis2016 |
| Central_LBK_EN | I0026 | Mathieson2015,Lazaridis2016 |
| Central_LBK_EN | I0046 | Mathieson2015,Lazaridis2016 |
| Central_LBK_EN | I0048 | Mathieson2015,Lazaridis2016 |
| Central_LBK_EN | I0054 | Mathieson2015,Lazaridis2016 |
| Central_LBK_EN | I0056 | Mathieson2015,Lazaridis2016 |
| Central_LBK_EN | I0057 | Mathieson2015,Lazaridis2016 |
| Central_LBK_EN | I0100 | Mathieson2015,Lazaridis2016 |
| Central_LBK_EN | I0659 | Mathieson2015,Lazaridis2016 |
| Central_LBK_EN | I0795 | Mathieson2015,Lazaridis2016 |
| Central_LBK_EN | I0797 | Mathieson2015,Lazaridis2016 |

| | | |
|---|---|---|
| Central_LBK_EN | I0821 | Mathieson2015,Lazaridis2016 |
| Central_LBK_EN | I1550 | Mathieson2015,Lazaridis2016 |
| Central_LBK_EN | LBK | Lazaridis2014 |
| MA1 | MA1 | Raghavan2014 |
| Other | I0114 | Mathieson2015,Lazaridis2016 |
| Other | I0122 | Mathieson2015,Lazaridis2016 |
| Other | I0126 | Mathieson2015,Lazaridis2016 |
| Other | I0232 | Mathieson2015,Lazaridis2016 |
| Other | I0234 | Mathieson2015,Lazaridis2016 |
| Other | I0235 | Mathieson2015,Lazaridis2016 |
| Other | I0246 | Mathieson2015,Lazaridis2016 |
| Other | I0247 | Mathieson2015,Lazaridis2016 |
| Other | I0354 | Mathieson2015,Lazaridis2016 |
| Other | I0358 | Mathieson2015,Lazaridis2016 |
| Other | I0359 | Mathieson2015,Lazaridis2016 |
| Other | I0360 | Mathieson2015,Lazaridis2016 |
| Other | I0361 | Mathieson2015,Lazaridis2016 |
| Other | I0371 | Mathieson2015,Lazaridis2016 |
| Other | I0374 | Mathieson2015,Lazaridis2016 |
| Other | I0411 | Mathieson2015,Lazaridis2016 |
| Other | I0418 | Mathieson2015,Lazaridis2016 |
| Other | I0419 | Mathieson2015,Lazaridis2016 |
| Other | I0421 | Mathieson2015,Lazaridis2016 |
| Other | I0422 | Mathieson2015,Lazaridis2016 |
| Other | I0423 | Mathieson2015,Lazaridis2016 |
| Other | I0424 | Mathieson2015,Lazaridis2016 |
| Other | I0430 | Mathieson2015,Lazaridis2016 |
| Other | I0431 | Mathieson2015,Lazaridis2016 |
| Other | I0432 | Mathieson2015,Lazaridis2016 |
| Other | I0433 | Mathieson2015,Lazaridis2016 |
| Other | I0434 | Mathieson2015,Lazaridis2016 |
| Other | I0440 | Mathieson2015,Lazaridis2016 |
| Other | I0725 | Mathieson2015,Lazaridis2016 |
| Other | I0854 | Mathieson2015,Lazaridis2016 |
| Other | I0861 | Mathieson2015,Lazaridis2016 |
| Other | I0867 | Mathieson2015,Lazaridis2016 |
| Other | I1069 | Mathieson2015,Lazaridis2016 |
| Other | I1072 | Mathieson2015,Lazaridis2016 |
| Other | I1274 | Mathieson2015,Lazaridis2016 |
| Other | I1290 | Mathieson2015,Lazaridis2016 |
| Other | I1293 | Mathieson2015,Lazaridis2016 |
| Other | I1302 | Mathieson2015,Lazaridis2016 |
| Other | I1407 | Mathieson2015,Lazaridis2016 |
| Other | I1409 | Mathieson2015,Lazaridis2016 |
| Other | I1414 | Mathieson2015,Lazaridis2016 |
| Other | I1415 | Mathieson2015,Lazaridis2016 |
| Other | I1416 | Mathieson2015,Lazaridis2016 |
| Other | I1530 | Mathieson2015,Lazaridis2016 |
| Other | I1541 | Mathieson2015,Lazaridis2016 |
| Other | I1584 | Mathieson2015,Lazaridis2016 |
| Other | I1631 | Mathieson2015,Lazaridis2016 |
| Other | I1632 | Mathieson2015,Lazaridis2016 |
| Other | I1633 | Mathieson2015,Lazaridis2016 |
| Other | I1634 | Mathieson2015,Lazaridis2016 |
| Other | I1635 | Mathieson2015,Lazaridis2016 |
| Other | I1656 | Mathieson2015,Lazaridis2016 |
| Other | I1658 | Mathieson2015,Lazaridis2016 |
| Other | I1661 | Mathieson2015,Lazaridis2016 |
| Other | I1662 | Mathieson2015,Lazaridis2016 |

| | | |
|---|---|---|
| Other | I1665 | Mathieson2015,Lazaridis2016 |
| Other | I1670 | Mathieson2015,Lazaridis2016 |
| Other | I1671 | Mathieson2015,Lazaridis2016 |
| Other | I1674 | Mathieson2015,Lazaridis2016 |
| Other | I1679 | Mathieson2015,Lazaridis2016 |
| Other | I1685 | Mathieson2015,Lazaridis2016 |
| Other | I1687 | Mathieson2015,Lazaridis2016 |
| Other | I1690 | Mathieson2015,Lazaridis2016 |
| Other | I1699 | Mathieson2015,Lazaridis2016 |
| Other | I1700 | Mathieson2015,Lazaridis2016 |
| Other | I1701 | Mathieson2015,Lazaridis2016 |
| Other | I1704 | Mathieson2015,Lazaridis2016 |
| Other | I1705 | Mathieson2015,Lazaridis2016 |
| Other | I1706 | Mathieson2015,Lazaridis2016 |
| Other | I1707 | Mathieson2015,Lazaridis2016 |
| Other | I1709 | Mathieson2015,Lazaridis2016 |
| Other | I1710 | Mathieson2015,Lazaridis2016 |
| Other | I1727 | Mathieson2015,Lazaridis2016 |
| Other | I1730 | Mathieson2015,Lazaridis2016 |
| Other | I1944 | Mathieson2015,Lazaridis2016 |
| Other | I1945 | Mathieson2015,Lazaridis2016 |
| Other | I1949 | Mathieson2015,Lazaridis2016 |
| Other | I1951 | Mathieson2015,Lazaridis2016 |
| Other | I1955 | Mathieson2015,Lazaridis2016 |
| Anatolia_Neolithic | Pal7 | Hofmanova2016 |
| Anatolia_Neolithic | Rev5 | Hofmanova2016 |
| Scandinavian_HG | I0011 | Haak2015,Mathieson2015 |
| Scandinavian_HG | I0012 | Haak2015,Mathieson2015 |
| Scandinavian_HG | I0013 | Haak2015,Mathieson2015 |
| Scandinavian_HG | I0014 | Haak2015,Mathieson2015 |
| Scandinavian_HG | I0015 | Haak2015,Mathieson2015 |
| Scandinavian_HG | I0017 | Haak2015,Mathieson2015 |
| Sweden_MN/TRB_MN | Gok2 | Skoglund2014 |
| Western_HG | Bichon | Jones2015 |
| Western_HG | I0585 | Haak2015,Mathieson2015 |
| Western_HG | I1507 | Haak2015,Mathieson2015 |
| Western_HG | Loschbour | Lazaridis2014 |
| Western_HG | Canes1 | Gonzales-Fortes2017 |
| Western_HG | Chan | Gonzales-Fortes2017 |
| Steppe_Yamnaya | I0231 | Haak2015,Mathieson2015 |
| Steppe_Yamnaya | I0357 | Haak2015,Mathieson2015 |
| Steppe_Yamnaya | I0370 | Haak2015,Mathieson2015 |
| Steppe_Yamnaya | I0429 | Haak2015,Mathieson2015 |
| Steppe_Yamnaya | I0438 | Haak2015,Mathieson2015 |
| Steppe_Yamnaya | I0439 | Haak2015,Mathieson2015 |
| Steppe_Yamnaya | I0441 | Haak2015,Mathieson2015 |
| Steppe_Yamnaya | I0443 | Haak2015,Mathieson2015 |
| Steppe_Yamnaya | I0444 | Haak2015,Mathieson2015 |
| Steppe_Yamnaya | RISE240 | Allentoft2015 |
| Steppe_Yamnaya | RISE546 | Allentoft2015 |
| Steppe_Yamnaya | RISE547 | Allentoft2015 |
| Steppe_Yamnaya | RISE548 | Allentoft2015 |
| Steppe_Yamnaya | RISE550 | Allentoft2015 |
| Steppe_Yamnaya | RISE552 | Allentoft2015 |

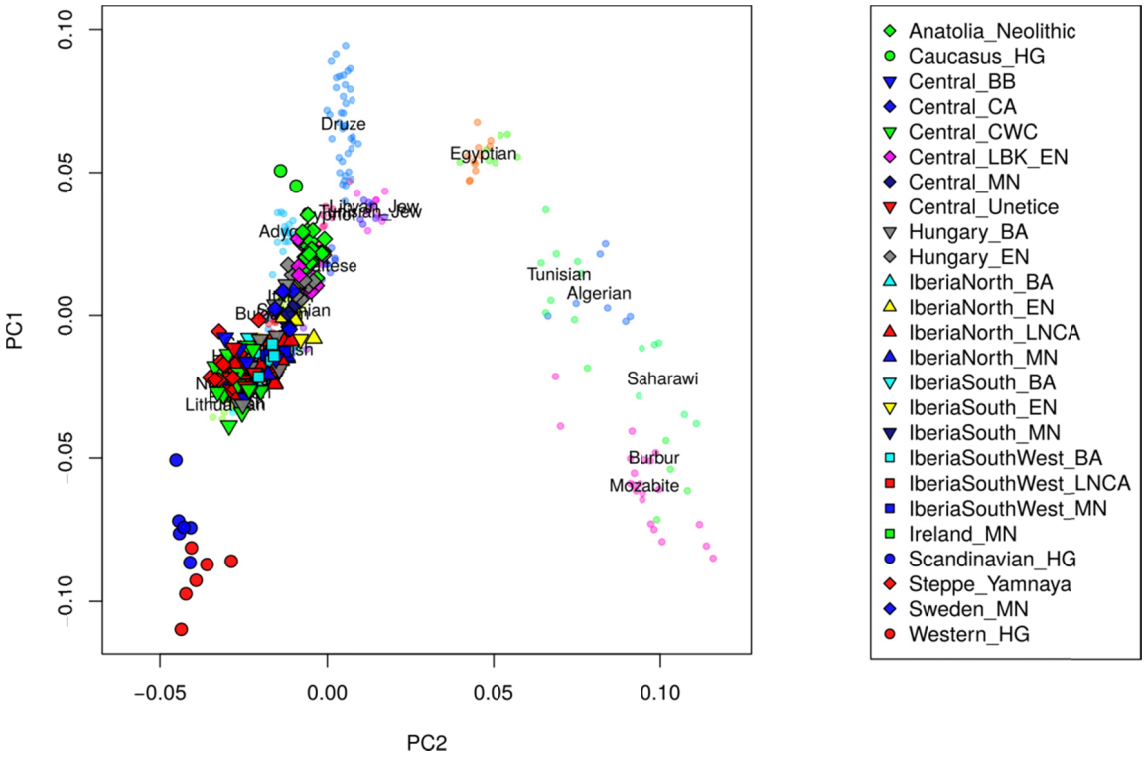


**Fig.S5.1**: PCA of ancient samples with modern European and North African populations. Model based clustering and estimation of ancestry proportions.

The model-based clustering approach implemented in *ADMIXTURE* (54) was run with all modern individuals of the Human Origins dataset and all ancient individuals. The data was LD pruned using *plink* v1.9(55, 56) using the parameters --indep-pairwise 200 25 0.4. Unsupervised *ADMIXTURE* was run for numbers of clusters K between 2 and 20 with 20 independent runs (different random seeds) per value of K. The lowest mean and median cross-validation error was obtained for K=16 (Figure S5.2). Common modes among the different runs were identified and clusters were aligned across different values of K using *pong* v1.4.6 (57) in greedy mode. Clustering results were then plotted in *GNU R*. The full *ADMIXTURE* results are shown in Dataset S3. In addition to this unsupervised approach we estimated the ancestry proportions attributable to early Anatolian farmers, hunter-gatherers and steppe herders (47, 58, 59) in Neolithic and Bronze Age Europeans by running supervised *ADMIXTURE*. Anatolian Neolithic farmers (50, 60, 61), Yamnaya herders (58, 59) and western hunter-gatherers were used as source populations. Common modes among 50 independent runs were identified and plotted using *pong* v1.4.6 (57) in greedy mode. The results of the supervised *ADMIXTURE* analysis is shown in Figure S5.3.

As an alternative approach to supervised *ADMIXTURE*, we used *ADMIXTOOLS qpAdm* v200 (48, 59) to estimate contributions of these three sources to Neolithic and Bronze Age European populations. Anatolian Neolithic farmers (50, 60, 61), Yamnaya herders (58, 59) and western hunter-gatherers were used as source populations and Ami_Coriell, BiakaPygmy, Bougainville, Chukchi, Eskimo_Naukan, Han, Karitiana, Kharia, Onge

from the Human Origins dataset as well as CHG (62) were used as outgroup populations. *qpAdm* was run on ancient populations using two sources (WHG and Anatolian Neolithic) for early and middle Neolithic as well as Chalcolithic populations, and all three sources for late Neolithic and Bronze Age groups.

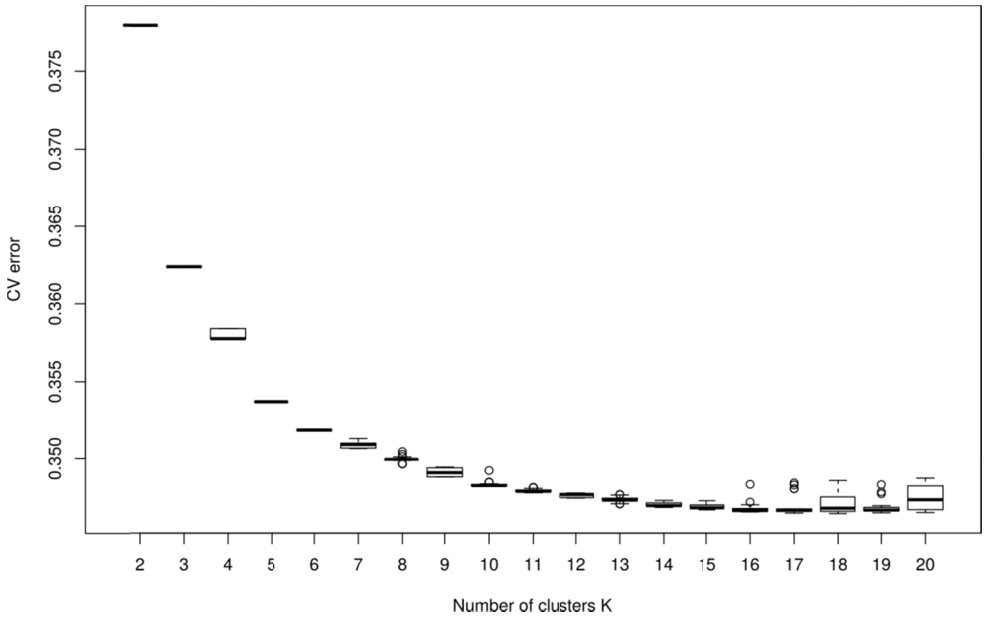


**Fig. S5.2**: Cross-validation error of the ADMIXTURE analysis represented as a box plot.

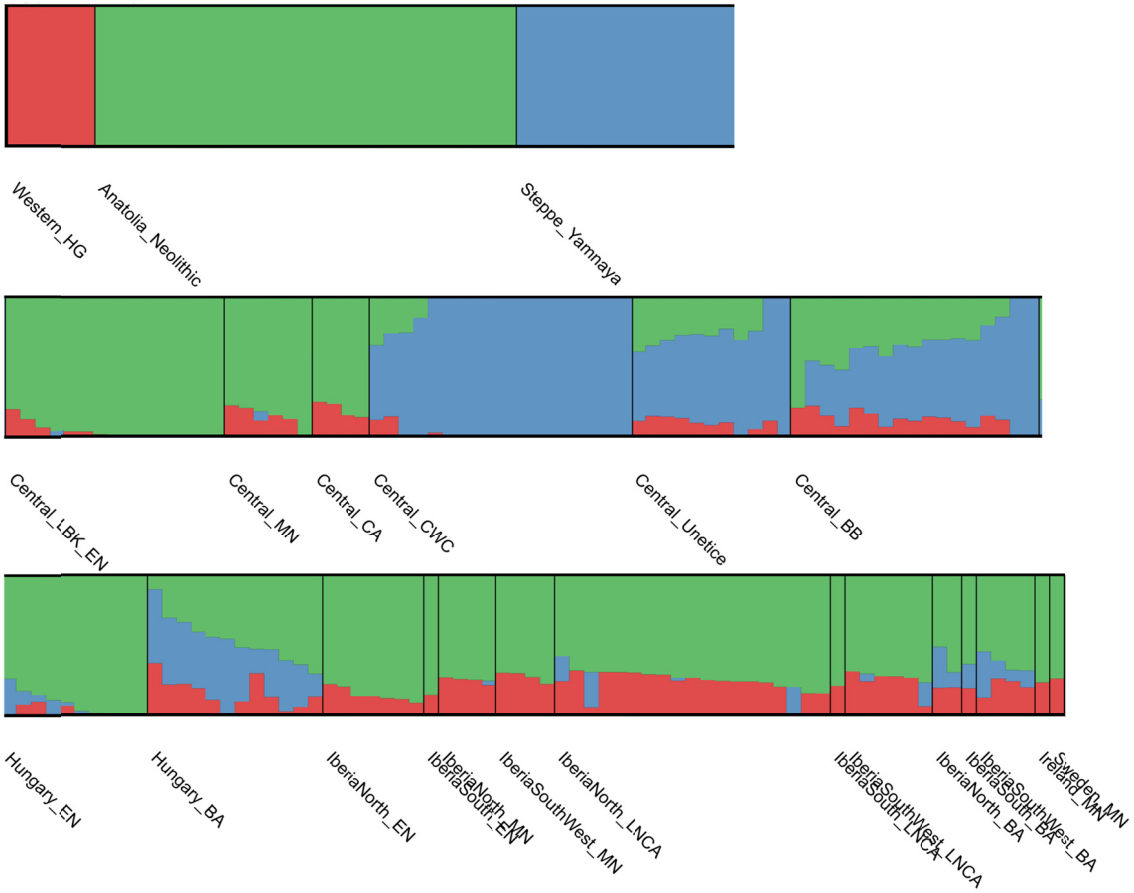


**Fig. S5.3**: Supervised ADMIXTURE results.

### *S5.4 f statistics and conditional nucleotide diversity*

Population affinities and shared drift among ancient individuals was measured using *D* and *f* statistics (48, 63) using *popstats* ((64), https://github.com/pontussk/popstats) and the captured SNP panel (50) to maximize the overlap between ancient individuals. Standard errors were estimated in a weighted block-jackknife procedure using blocks of 5Mb.

To assess diversity within populations, we calculated conditional nucleotide diversity (44) for prehistoric groups with at least two shotgun-sequenced individuals. The two highest coverage individuals per group were used for these calculations. For prehistoric Hungarians, we used the shotgun data published in (65) while we used SNP capture data (50) for the same individuals in all other analyses. This analysis was conducted using the 1000 genomes Yoruba (49) ascertained transversion SNPs to avoid effects of post-mortem damage and ascertainment bias. Standard errors were estimated using a block-jackknife and a block size of 2000 SNPs.

## References


1. Vera-Rodríguez JC & Gavilán-Ceballos B (1999) Organización interna y usos del espacio en la Cueva de los Murciélagos de Zuheros (Córdoba). *Sagvntum Extra* 2(Actes del II Congrés del Neolític a la Península Ibèrica. (Valéncia, 7-9 s'Abril)):229-234.
2. Vera Rodríguez JC*, et al.* (1999) Prehistoria. *Zuheros. Un recorrido por su pasado*, ed Molina Expósito A (Ayuntamiento de Zuheros,, Zuheros), pp 13-20.
3. Vera-Rodríguez JC*, et al.* (2014) Los contextos sepulcrales de la Cueva de los Cuarenta. Arqueología de los gestos funerarios durante la segunda mitad del IV milenio BC en el subbético cordobés. *Antiqvitas* 26:81-122.
4. Asquerino Fernández MD (1985) Sepultura argárica en Priego de Córdoba. *Boletín de la Real Academia de Córdoba* 56:183-188.
5. Arsuaga JL*, et al.* (2014) Neandertal roots: Cranial and chronological evidence from Sima de los Huesos. *Science* 344(6190):1358.
6. Bermu´dez de Castro JM*, et al.* (1999) The TD6 (Aurora stratum) hominid site. Final remarks and new questions. *J. Hum. Evol.* 37(3):695-700.
7. Carretero JM*, et al.* (2008) A Late Pleistocene-Early Holocene archaeological sequence of Portalón de Cueva Mayor (Sierra de Atapuerca, Burgos, Spain). *Munibe (Antropologia-Arkeologia)* 59:67-80.
8. Pérez-Romero A*, et al.* (2017) An unusual Pre-bell beaker copper age cave burial context from El Portalón de Cueva Mayor site (Sierra de Atapuerca, Burgos). *Quaternary International* 433:142-155.
9. Günther T*, et al.* (2015) Ancient genomes link early farmers from Atapuerca in Spain to modern-day Basques. *Proc. Natl. Acad. Sci. U. S. A.* 112(38):11917-11922.
10. Sverrisdottir OO*, et al.* (2014) Direct estimates of natural selection in Iberia indicate calcium absorption was not the only driver of lactase persistence in Europe. *Mol. Biol. Evol.* 31(4):975-983.
11. Anderung C*, et al.* (2005) Prehistoric contacts over the Straits of Gibraltar indicated by genetic analysis of Iberian Bronze Age cattle. *Proc. Natl. Acad. Sci. U. S. A.* 102(24):8431-8435.
12. Lira J*, et al.* (2010) Ancient DNA reveals traces of Iberian Neolithic and Bronze Age lineages in modern Iberian horses. *Mol. Ecol.* 19(1):64-78.
13. Wadsworth C*, et al.* (2017) Comparing ancient DNA survival and proteome content in 69 archaeological cattle tooth and bone samples from multiple European sites. *J. Proteomics* 158:1-8.
14. Casado López P & Hernández Vera JA (1979) Materiales del Bronce Final de la Cueva de los Lagos (Logroño). *Caesaraugusta* 47-48:97-125.

15. Hernández Vera JA (1983) Difusión de elementos de la cultura de Cogotas hacia el Valle del Ebro. *Cuadernos de investigación: Historia* 9(1):65-80,.
16. Alday A (2012) Treviño, un paraíso en la Prehistoria. *Viaje a Íbita. Estudios Históricos Del Condado de Treviño*, eds González de Viñaspe R & Garay Osma R (Ayuntamiento del Condado de Treviño, Treviño), pp 48-70.
17. Alday A*, et al.* (2009) *Reflejos del Neolítico Ibérico. La Cerámica Boquique: Caracteres, cronología y Contexto.* (EDAR. Arqueologia y Patrimonio, Milano) p 179.
18. Alday A, Gundín E, López de Heredia J, Soto A, & Tarriño A (2008) El túmulo funerario Neolítico de San Quílez. San Martín Zar-Treviño: un dispositivo y unos ritos originales en el cuarto milenio a.C. *MUNIBE (Antropología y Arqueología)* 59:133–156.
19. Dabney J*, et al.* (2013) Complete mitochondrial genome sequence of a Middle Pleistocene cave bear reconstructed from ultrashort DNA fragments. *Proc. Natl. Acad. Sci. U. S. A.* 110(39):15758-15763.
20. Meyer M & Kircher M (2010) Illumina sequencing library preparation for highly multiplexed target capture and sequencing. *Cold Spring Harbor protocols* 2010(6).
21. Fontanals-Coll M, Díaz-Zorita Bonilla M, & Subirà ME (2016) A Palaeodietary Study of Stable Isotope Analysis from a High-status Burial in the Copper Age: The Montelirio Megalithic Structure at Valencina de la Concepción–Castilleja de Guzmán, Spain. *International Journal of Osteoarchaeology* 26(3):447-459.
22. Fontanals-Coll M, Eulàlia Subirà M, Díaz-Zorita Bonilla M, & Gibaja JF (2017) First insight into the Neolithic subsistence economy in the north-east Iberian Peninsula: paleodietary reconstruction through stable isotopes. *Am. J. Phys. Anthropol.* 162(1):36-50.
23. Fontanals-Coll M, Subirà ME, Bonilla MD-Z, Duboscq S, & Gibaja JF (2015) Investigating palaeodietary and social differences between two differentiated sectors of a Neolithic community, La Bòbila Madurell-Can Gambús (north-east Iberian Peninsula). *Journal of Archaeological Science: Reports* 3:160-170.
24. Lubell D, Jackes M, Schwarcz H, Knyf M, & Meiklejohn C (1994) The Mesolithic-Neolithic Transition in Portugal: Isotopic and Dental Evidence of Diet. *Journal of Archaeological Science* 21(2):201-216.
25. McClure SB, García O, Roca de Togores C, Culleton BJ, & Kennett DJ (2011) Osteological and paleodietary investigation of burials from Cova de la Pastora, Alicante, Spain. *Journal of Archaeological Science* 38(2):420-428.
26. Waterman AJ, Tykot RH, & Silva AM (2016) Stable Isotope Analysis of Diet-based Social Differentiation at Late Prehistoric Collective Burials in South-Western Portugal. *Archaeometry* 58(1):131-151.
27. Carvalho AF & Petchey F (2013) Stable Isotope Evidence of Neolithic Palaeodiets in the Coastal Regions of Southern Portugal. *The Journal of Island and Coastal Archaeology* 8(3):361-383.
28. Webb EC*, et al.* (2017) The influence of varying proportions of terrestrial and marine dietary protein on the stable carbon-isotope compositions of pig tissues from a controlled feeding experiment. *STAR: Science & Technology of Archaeological Research* 3(1):36-52.
29. Webb EC*, et al.* (2015) Compound-specific amino acid isotopic proxies for detecting freshwater resource consumption. *Journal of Archaeological Science* 63:104-114.
30. Honch NV, McCullagh JSO, & Hedges REM (2012) Variation of bone collagen amino acid δ13c values in archaeological humans and fauna with different dietary regimes: Developing frameworks of dietary discrimination. *Am. J. Phys. Anthropol.* 148(4):495-511.
31. Longin R (1971) New Method of Collagen Extraction for Radiocarbon Dating. *Nature* 230(5291):241-242.
32. Richards MP & Hedges REM (1999) Stable Isotope Evidence for Similarities in the Types of Marine Foods Used by Late Mesolithic Humans at Sites Along the Atlantic Coast of Europe. *Journal of Archaeological Science* 26(6):717-722.
33. Mora A*, et al.* (2017) High-resolution palaeodietary reconstruction: Amino acid δ13C analysis of keratin from single hairs of mummified human individuals. *Quaternary International* 436, Part A:96-113.
34. Smith CI, Fuller BT, Choy K, & Richards MP (2009) A three-phase liquid chromatographic method for δ13C analysis of amino acids from biological protein hydrolysates using liquid chromatography–isotope ratio mass spectrometry. *Anal. Biochem.* 390(2):165-172.
35. Reimer P*, et al.* (2013) IntCal13 and Marine13 radiocarbon age calibration curves 0–50,000 years cal BP. *Radiocarbon* 55(4):1869–1887.
36. Kircher M (2012) Analysis of high-throughput ancient DNA sequencing data. *Methods Mol. Biol.* 840:197–228.

37. Li H & Durbin R (2009) Fast and accurate short read alignment with Burrows-Wheeler transform. *Bioinformatics (Oxford, England)* 25(14):1754-1760.
38. Günther T, *et al.* (2018) Genomics of Mesolithic Scandinavia reveal colonization routes and high-latitude adaptation. *PLoS Biol*. 16(1): e200370.
39. Li H, *et al.* (2009) The Sequence Alignment/Map format and SAMtools. *Bioinformatics (Oxford, England)* 25(16):2078-2079.
40. Skoglund P, Storå J, Götherström A, & Jakobsson M (2013) Accurate sex identification of ancient human remains using DNA shotgun sequencing. *Journal of Archaeological Science* 40(12):4477-4482.
41. Green RE, *et al.* (2008) A complete Neandertal mitochondrial genome sequence determined by high-throughput sequencing. *Cell* 134(3):416-426.
42. Rasmussen M, *et al.* (2011) An Aboriginal Australian genome reveals separate human dispersals into Asia. *Science (New York, N.Y.)* 334(6052):94-98.
43. Korneliussen TS, Albrechtsen A, & Nielsen R (2014) ANGSD: Analysis of Next Generation Sequencing Data. *BMC Bioinformatics* 15(1):356.
44. Skoglund P, *et al.* (2014) Genomic diversity and admixture differs for Stone-Age Scandinavian foragers and farmers. *Science* 344(6185):747-750.
45. Vianello D, *et al.* (2013) HAPLOFIND: A New Method for High-Throughput mtDNA Haplogroup Assignment. *Hum. Mutat.* 34(9):1189-1194.
46. van Oven M, Van Geystelen A, Kayser M, Decorte R, & Larmuseau M (2014) Seeing the wood for the trees: a minimal reference phylogeny for the human Y chromosome. . *Hum. Mutat.* 35(2):187-191.
47. Lazaridis I, *et al.* (2014) Ancient human genomes suggest three ancestral populations for present-day Europeans. *Nature* 513(7518):409-413.
48. Patterson NJ, *et al.* (2012) Ancient Admixture in Human History. *Genetics* 192:1065-1093.
49. Consortium TGP (2012) An integrated map of genetic variation from 1,092 human genomes. *Nature* 491(7422):56-65.
50. Mathieson I, *et al.* (2015) Genome-wide patterns of selection in 230 ancient Eurasians. *Nature* 528(7583):499-503.
51. Patterson N, Price AL, & Reich D (2006) Population Structure and Eigenanalysis. *PLoS Genet* 2(12).
52. Skoglund P, *et al.* (2012) Origins and genetic legacy of Neolithic farmers and hunter-gatherers in Europe. *Science* 336(6080):466-469.
53. Wang C, *et al.* (2010) Comparing Spatial Maps of Human Population-Genetic Variation Using Procrustes Analysis. *Stat. Appl. Genet. Mol. Biol.* 9(1):Article 13.
54. Alexander DH, Novembre J, & Lange K (2009) Fast model-based estimation of ancestry in unrelated individuals. *Genome Res.* 19:1655–1664.
55. Purcell S, *et al.* (2007) PLINK: a tool set for whole-genome association and population-based linkage analyses. *Am. J. Hum. Genet.* 81(3):559-575.
56. Chang W, Cathcart C, Hall D, & Garrett A (2015) Ancestry-Constrained Phylogenetic Analysis supports the Indo-European Steppe Hypothesis. *Language* 91(1):194-244.
57. Behr AA, Liu KZ, Liu-Fang G, Nakka P, & Ramachandran S (2016) pong: fast analysis and visualization of latent clusters in population genetic data. *Bioinformatics* 32(18):2817-2823.
58. Allentoft ME, *et al.* (2015) Population genomics of Bronze Age Eurasia. *Nature* 522(7555):167-172.
59. Haak W, *et al.* (2015) Massive migration from the steppe was a source for Indo-European languages in Europe. *Nature* 522:207-211.
60. Omrak A, *et al.* (2016) Genomic Evidence Establishes Anatolia as the Source of the European Neolithic Gene Pool. *Curr. Biol.* 26(2):270-275.
61. Hofmanova Z, *et al.* (2016) Early farmers from across Europe directly descended from Neolithic Aegeans. *Proc. Natl. Acad. Sci. U. S. A.* 113(25):6886-6891.
62. Jones ER, *et al.* (2015) Upper Palaeolithic genomes reveal deep roots of modern Eurasians. *Nature communications* 6:8912.
63. Reich D, Thangaraj K, Patterson N, Price AL, & Singh L (2009) Reconstructing Indian population history. *Nature* 461(7263):489-494.
64. Skoglund P, *et al.* (2015) Genetic evidence for two founding populations of the Americas. *Nature* 525(7567):104-108.
65. Gamba C, *et al.* (2014) Genome flux and stasis in a five millennium transect of European prehistory. *Nature communications* 5:5257.